DMD DRUG METABOLISM AND DISPOSITION aspet

was recorded by using a 1420 ARVO MX luminometer (PerkinElmer Life and Analytical Sciences–Wallac Oy, Turku, Finland).

Detection of Semicarbazide Adducts. A typical reaction mixture (final volume of 0.5 ml) contained 100 nM human CYP2C9 or CYP3A4 Supersomes, 50 mM potassium phosphate buffer (pH 7.4), 1 mM NADPH, 10 mM semicarbazide, and 20 μM [^{14}C]losartan. The final concentration of ethanol in the reaction mixture was less than 1%. Incubation was performed at 37°C for 60 min and terminated by addition of 2 ml of ice-cold methanol. After centrifugation at 15,000*g*, the supernatant was subjected to liquid chromatography (LC)-tandem mass spectrometry (MS/MS) (4000 QTRAP; Applied Biosystems, Foster City, CA). An Agilent 1200 (Agilent Technologies, Santa Clara, CA) was used as the liquid chromatograph with an Inertsil ODS-3V column (5-μm particle size, 4.6 mm i.d. × 250 mm; GL Science, Inc., Tokyo, Japan). The column temperature was 40°C. The mobile phase was 10 mM ammonium acetate buffer (A) and acetonitrile (B). The conditions for elution were as follows: 5 to 45% B (0–5 min), 45 to 70% B (5–55 min), 70 to 100% B (55–60 min), and 5% B (60.01–70 min). Linear gradients were used for all solvent changes. The flow rate was 1 ml/min. The liquid chromatograph was connected to a 4000 QTRAP mass spectrometer operated by the enhanced product ion under the positive mode. The turbo gas was maintained at 450°C. Air was used as the nebulizing and turbo gas at 50 psi. Nitrogen was used as the curtain gas at 30 psi. The declustering potential and collision energy were 50 V and 20 V, respectively. The *m/z* 150 to 500 was scanned at the precursor ion (*m/z* 494.2; semicarbazide adducts of losartan hydroxide).

Identification of Semicarbazide Adducts. A liquid chromatography ion trap time-of-flight mass spectrometry (LCMS-IT-TOF) system (Shimadzu, Kyoto, Japan) was used to identify the structures of the semicarbazide adducts of the losartan hydroxide. The incubation mixture was the same as described above. After centrifugation at 15,000*g* for 5 min, the supernatant was subjected to LCMS-IT-TOF using an Inertsil ODS-3 analytical column (5-μm particle size, 4.6 mm i.d. × 250 mm). The LC conditions were the same as described earlier.

Statistical Methods. Data are expressed as means ± S.D. Statistical significance between the two groups was determined by a two-tailed Student's *t* test. $P < 0.05$ was considered statistically significant.

Results

MOI- and Time-Dependent Changes of Diclofenac 4′-Hydroxylase Activity and CYP2C9 Protein Level. To investigate the optimum multiplicity of infection (MOI), HepG2 cells were infected with AdCYP2C9 at MOI 0, 2.5, 5, 10, or 20 for 2 days. Diclofenac 4′-hydroxylase activity and CYP2C9 protein level were measured (Fig. 1). The activity and CYP2C9 protein level were increased MOI dependently in AdCYP2C9-infected cells, whereas they were not detected in AdGFP-infected cells at MOI 20. The highest activity and protein level were observed in cells infected with AdCYP2C9 at MOI 20, but the cells were slightly damaged (data not shown). At MOI 10, diclofenac 4′-hydroxylase activity was 0.957 ± 0.070 nmol/min/mg protein, a value that was higher than those in human hepatocytes reported in other reports (Supplemental Table 1). With HepG2 cells infected with AdCYP2C9 at MOI 10 for 1, 2, 3, or 5 days, the highest activity was observed after a 2-day infection, although the protein levels appeared to be similar after 2- to 5-day infections (Fig. 1B). From these results, AdCYP2C9 infection to HepG2 cells was performed at MOI 10 for 2 days in the subsequent experiments.

Effect of SiNrf2 on Nrf2 Protein Expression in Adenovirus-Infected HepG2 Cells. Our recent study demonstrated that CYP3A4-induced cytotoxicities of several drugs such as acetaminophen and flutamide were sensitively detected by Nrf2 knockdown (H. Hosomi, T. Fukami, A Iwamura, M. Nakajima, and T. Yokoi, manuscript submitted for publication). This study also used HepG2 cells transfected with siNrf2. Nrf2 protein expression in HepG2 cells was efficiently decreased by transfection of siNrf2 (26.8 ± 1.1 and 27.1 ± 2.0%, respectively), and the effect of siNrf2 was not affected by CYP2C9 overexpression (Fig. 1C).

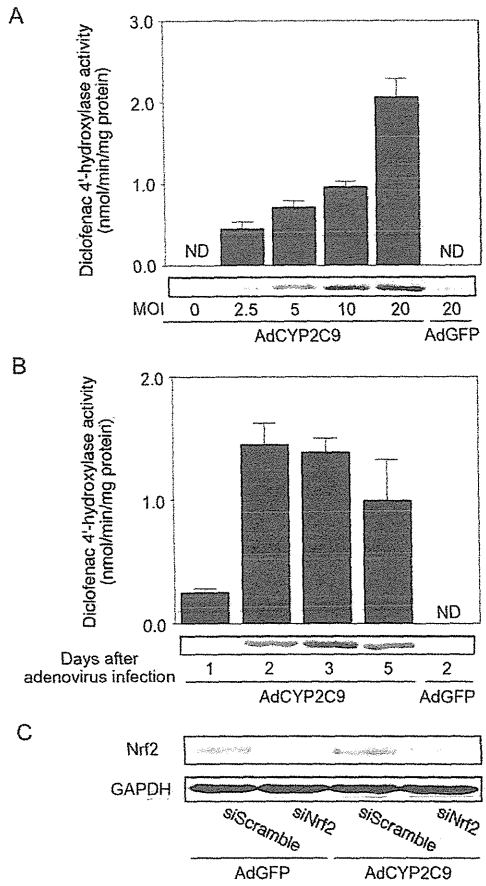

FIG. 1. MOI-dependent (A) and time-dependent (B) changes of diclofenac 4′-hydroxylase activity and CYP2C9 protein level in adenovirus (AdCYP2C9 or AdGFP)-infected HepG2 cells. HepG2 cells were infected with adenovirus for 2 days (A) or at MOI 10 (B). Diclofenac 4′-hydroxylase activity was measured as described under *Materials and Methods*. The CYP2C9 protein level was analyzed by immunoblotting using total cell homogenates from adenovirus-infected HepG2 cells, and the representative bands are demonstrated. Data are means ± S.D. (n = 3). C, Nrf2 protein level in HepG2 cells transfected with siScramble or siNrf2. HepG2 cells were infected with adenovirus (AdCYP2C9 or AdGFP) at MOI 10 for 2 days after a 24-h incubation with 10 nM siRNA. The relative band intensity of Nrf2 was normalized with the band intensity of GAPDH. Data are means ± S.D. (n = 3). **, $P < 0.01$ compared with AdGFP-infected groups transfected with siScramble. ND, not detected.

CYP2C9-Induced Cytotoxicity in HepG2 Cells Transfected with siNrf2. To investigate the CYP2C9-mediated metabolic activation of eight hepatotoxic drugs (benzbromarone, flutamide, fluvastatin, losartan, terbinafine, tienilic acid, valproic acid, and zolpidem), HepG2 cells infected with AdCYP2C9 at MOI 10 for 2 days were treated with drugs for 24 h. As a negative control, AdGFP was infected at MOI 10. To improve the sensitivity, HepG2 cells were transfected with siNrf2 24 h before adenovirus infection. Cytotoxicity was evaluated by WST-8 and ATP assays (Figs. 2 and 3). In the WST-8 assay, the viabilities of AdCYP2C9-infected cells were significantly decreased compared with those of AdGFP-infected cells by treatment with benzbromarone (10–40 μM), tienilic acid (100 and 200 μM), and losartan (25–100 μM) (Fig. 2). On the other hand, the viabilities of AdCYP2C9-infected cells were not different from those of AdGFP-infected cells by treatment with flutamide, fluvastatin, terbinafine, valproic acid, and zolpidem, except when treated with 100 μM fluvastatin. The ATP assay revealed a result similar to that of the WST-8 assay in that the viabilities of AdCYP2C9-infected cells were significantly decreased compared with those of AdGFP-infected cells by treatment with the benzbromarone (10–40 μM), tienilic acid

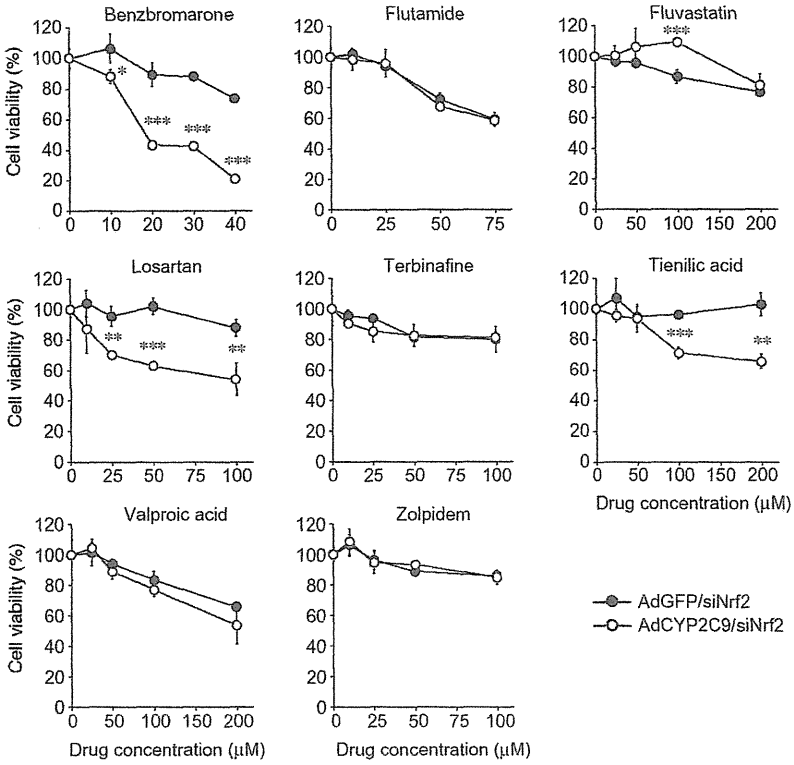

FIG. 2. CYP2C9-induced cytotoxicity in HepG2 cells transfected with siNrf2 (WST-8 assay). HepG2 cells were infected with adenovirus at MOI 10 for 2 days after a 24-h incubation with 10 nM siNrf2. Cell viability was measured by WST-8 assay after a 24-h treatment with the test drugs. Cell viability is expressed as a percentage of cells without drug treatment. Data are means ± S.D. ($n = 3$). *, $P < 0.05$; **, $P < 0.01$; ***, $P < 0.001$, compared with AdGFP-infected groups.

(50–200 μM), and losartan (10–100 μM) (Fig. 3). These results suggested that the benzbromarone-, tienilic acid-, and losartan-induced cytotoxicities are caused by the metabolic activation of CYP2C9.

CYP2C9-Induced Cytotoxicity in HepG2 Cells Transfected with siScramble. To investigate whether Nrf2-associated cytoprotective genes were involved in the benzbromarone-, tienilic acid-, and losartan-induced cytotoxicities mediated by CYP2C9, the cytotoxicity was evaluated with HepG2 cells transfected with siScramble instead of siNrf2 (Fig. 4). Terbinafine was used as a negative control. With the drugs except terbinafine, the viabilities of AdCYP2C9-infected cells were significantly decreased compared with those of AdGFP-

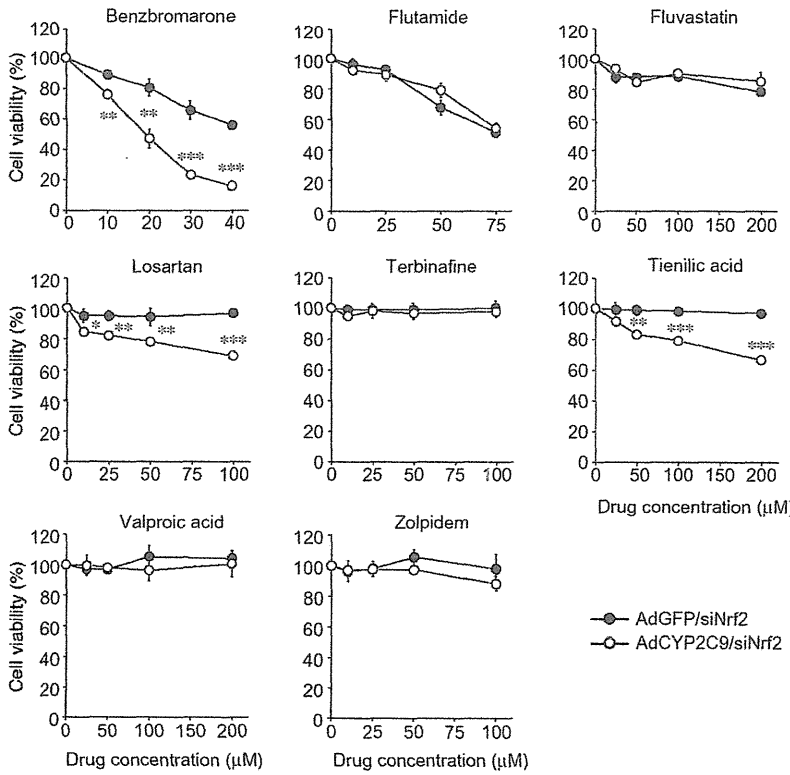

FIG. 3. CYP2C9-induced cytotoxicity in HepG2 cells transfected with siNrf2 (ATP assay). HepG2 cells were infected with adenovirus at MOI 10 for 2 days after a 24-h incubation with 10 nM siNrf2. Cell viability was measured by ATP assay after a 24-h treatment with the test drugs. Cell viability is expressed as a percentage of cells without drug treatment. Data are means ± S.D. ($n = 3$). *, $P < 0.05$; **, $P < 0.01$; ***, $P < 0.001$, compared with AdGFP-infected groups.

DRUG METABOLISM AND DISPOSITION DMD aspet
Downloaded from dmd.aspetjournals.org at Kanazawa Univ Yakugakubu Lib on May 2, 2011

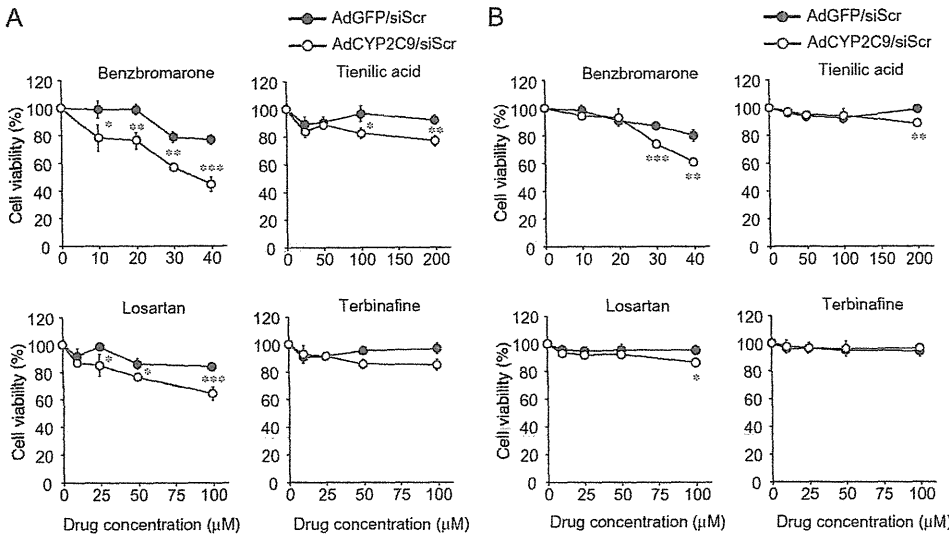

FIG. 4. CYP2C9-induced cytotoxicity in HepG2 cells transfected with siScramble. HepG2 cells were infected with adenovirus at MOI 10 for 2 days after a 24-h transfection with 10 nM siScramble. Cell viability was measured by the WST-8 assay (A) and the ATP assay (B) after a 24-h treatment with the test drugs. Cell viability is expressed as a percentage of cells without drug treatment. Data are means ± S.D. ($n = 3$). *, $P < 0.05$; **, $P < 0.01$; ***, $P < 0.001$, compared with AdGFP-infected groups.

infected cells, but the differences in the viabilities between AdGFP- and AdCYP2C9-infected cells transfected with siScramble were less than those of cells transfected with siNrf2.

Comparison of CYP2C9-Mediated Cytotoxicity between Losartan and Various Sartans. Because the cell-based assay system revealed that the losartan-induced cytotoxicity involved metabolic activation by CYP2C9, it was conceivable that other sartans with similar structures were also metabolically activated by CYP2C9. The viabilities of AdCYP2C9-infected cells were investigated by treatment with various sartans such as eprosartan, candesartan, irbesartan, olmesartan, telmisartan, and valsartan. However, no sartans other than losartan affected the cell viabilities (Fig. 5). Thus, among members of the sartan family, only losartan is associated with CYP2C9-mediated cytotoxicity.

Detection of Semicarbazide Adducts of Losartan. The semicarbazide adducts of losartan were investigated by the positive ion mode of LC-MS/MS. It was reported that CYP3A4 is involved in the metabolism of losartan (Stearns et al., 1995). However, no cytotoxicity of losartan was induced when the cells were infected with AdCYP3A4 constructed previously (Hosomi et al., 2010) instead of AdCYP2C9 (data not shown). Therefore, to detect adducts specifically generated by CYP2C9, losartan was incubated with CYP2C9 or CYP3A4 (negative control) Supersomes. As shown in Fig. 6, three semicarbazide adducts of losartan (S1, S2, and S3) were detected in the presence of CYP2C9 Supersomes by a precursor ion scan at *m/z* 494.2 ($[M + H]^+$). Because S3 was also detected when incubated with the CYP3A4 Supersomes, S3 was considered not to be involved in the CYP2C9-mediated cytotoxicity. Therefore, the subsequent study of S3 was not performed.

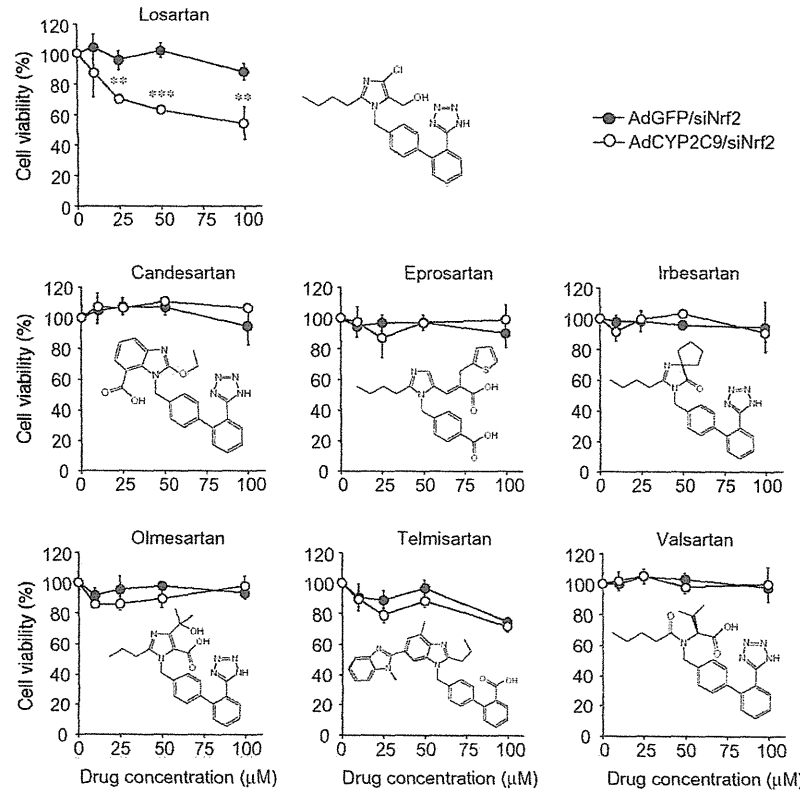

FIG. 5. Comparison of CYP2C9-mediated cytotoxicity between losartan and various sartans. HepG2 cells were infected with adenovirus at MOI 10 for 2 days after a 24-h transfection with 10 nM siNrf2. Cell viability was measured by the WST-8 assay after a 24-h treatment with the drugs. Cell viability is expressed as a percentage of cells without drug treatment. Data are means ± S.D. ($n = 3$). *, $P < 0.05$; **, $P < 0.01$, compared with AdGFP-infected groups.

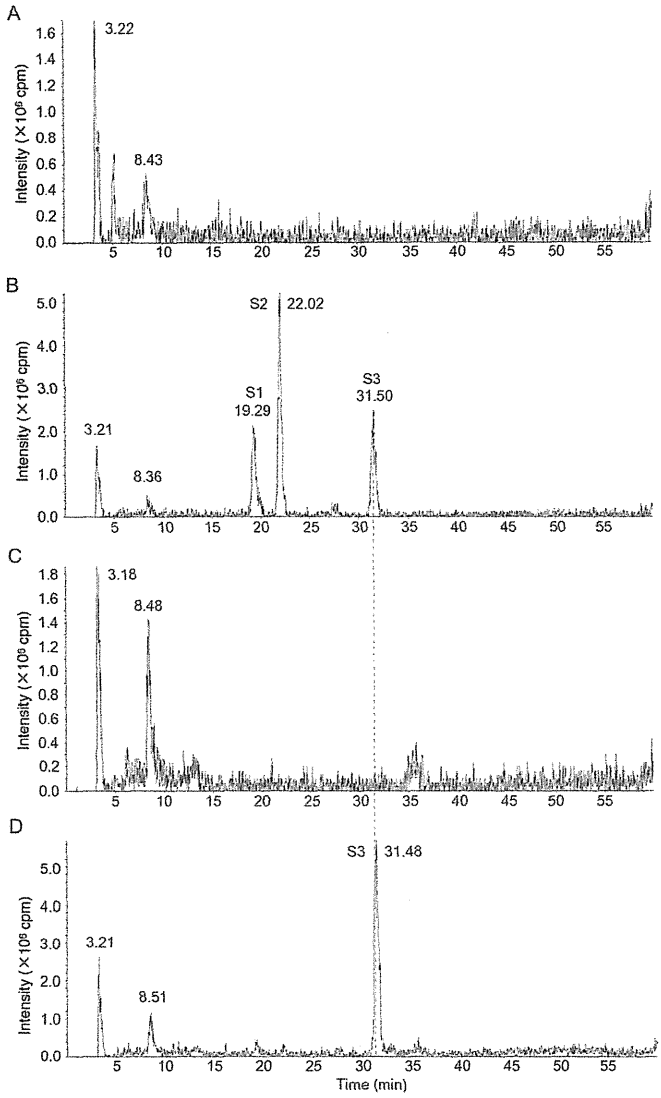

FIG. 6. Ion chromatograms from LC-MS/MS analysis of the semicarbazide adducts of losartan at *m/z* 494.2 ($[M + H]^+$). A, CYP2C9 Supersomes without semicarbazide. B, CYP2C9 Supersomes with semicarbazide. C, CYP3A4 Supersomes without semicarbazide. D, CYP3A4 Supersomes with semicarbazide. Incubation and LC-MS/MS conditions were as described under *Materials and Methods*.

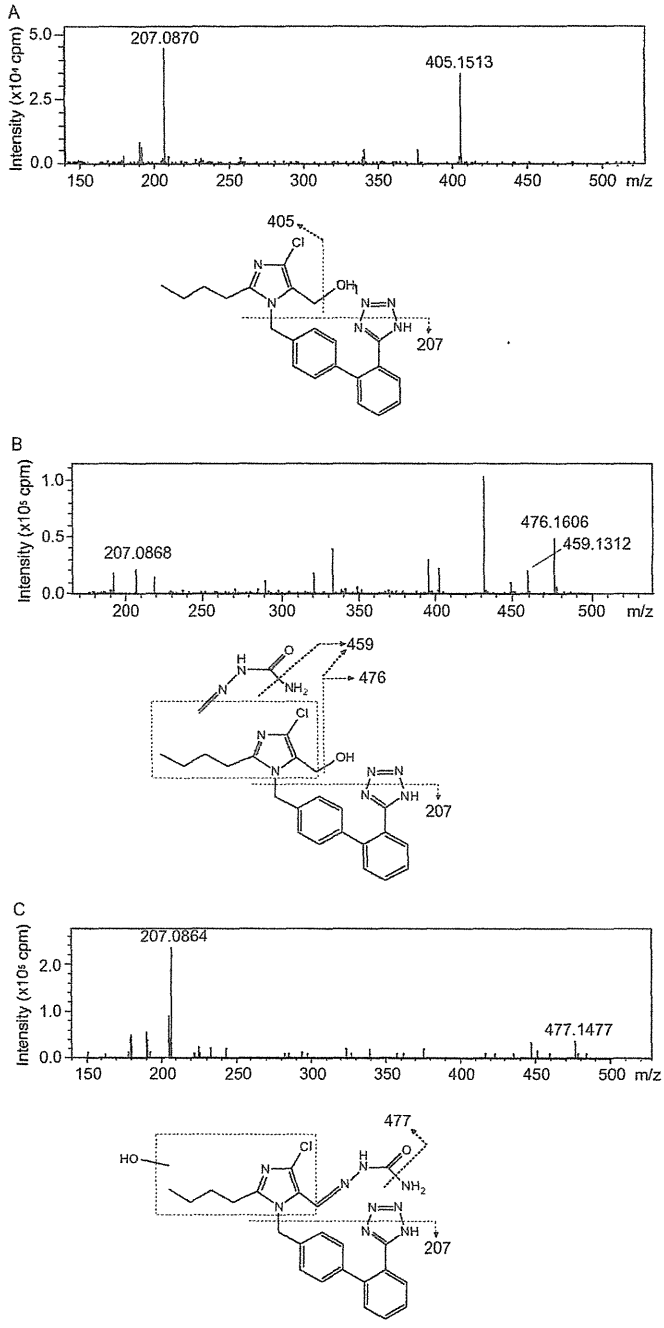

FIG. 7. Predicted structures of semicarbazide adducts of losartan and MS/MS spectra of the product ion obtained by collision-induced dissociation of (A) losartan at *m/z* 423.2 ($[M + H]^+$) and (B) S1 and (C) S2 at *m/z* 494.2 ($[M + H]^+$). The precursor ion at *m/z* 423.2 is semicarbazide adducts of losartan hydroxide. These spectra were scanned using LCMS-IT-TOF. Incubation and LCMS-IT-TOF conditions were as described under *Materials and Methods*.

Identification of Semicarbazide Adducts of Losartan. The structures of S1 and S2 were estimated by the positive ion mode of LCMS-IT-TOF (Fig. 7). The product ion mass spectrum of losartan exhibited a major fragment ion at *m/z* 405.1513 ($C_{22}H_{22}N_6Cl$) (Fig. 7A). The fragment ion at *m/z* 405.1513 was $[M + H - 18]^+$, indicating the losses of H_2O from alcohol group of losartan. The product ion mass spectrum of S1 exhibited two major fragment ions at *m/z* 476.1606 ($C_{23}H_{23}N_9OCl$) and *m/z* 459.1312 ($C_{23}H_2ON_8OCl$). The fragment ions at *m/z* 476.1606 and *m/z* 459.1312 were $[M + H - 18]^+$ and $[M + H - 35]^+$, indicating the losses of H_2O and NH_3 and H_2O, respectively. On the other hand, the product ion mass spectrum of S2 exhibited fragment ions at *m/z* 477.1477. The fragment ions at *m/z* 477.1477 were $[M + H - 17]^+$, indicating the loss of NH_3 from semicarbazide. Furthermore, the fragment ion at *m/z* 207.08 given from all three precursor ions indicated no conjugation with the biphenyl or tetrazole ring. The possible structures of S1 and S2 are shown in Fig. 7, B and C. *m/z* 207.08 indicated no conjugation with the biphenyl or tetrazole ring, and $[M + H - 18]^+$ indicated the losses of H_2O from alcohol group of losartan. Therefore, these two fragment ions detected in both losartan and S1 suggested that semicarbazide conjugates with another position, that is, somewhere in the imidazole ring or the adjacent butyl side chain. In contrast, $[M + H - 17]^+$ instead of $[M + H - 18]^+$ given from S2 suggested that a reactive metabolite conjugated with semicarbazide is a hydroxylated form of E3179, an aldehyde metabolite of losartan.

Discussion

In this study, we constructed an in vitro cell-based assay system to evaluate the hepatotoxicity mediated by CYP2C9 and performed a

DMD DRUG METABOLISM AND DISPOSITION aspet
Downloaded from dmd.aspetjournals.org at Kanazawa Univ Yakugakubu Lib on May 2, 2011

DMD DRUG METABOLISM AND DISPOSITION aspet

cytotoxicity assay for drugs that have been known to cause hepatotoxicity. Benzbromarone and tienilic acid are converted to reactive metabolites by CYP2C9. In addition, six other hepatotoxic drugs, whose reactive metabolites generated by CYP2C9 have not been identified although CYP2C9 is involved in their metabolism, were evaluated by our cell-based assay system. According to O'Brien et al. (2006), the cytotoxicity assay was performed within the drug concentration of 30 times the maximal efficacious concentration or 100 μM. We found that the viabilities of AdCYP2C9-infected cells were significantly decreased compared with those of AdGFP-infected cells by treatments with benzbromarone, tienilic acid, and losartan, suggesting that the hepatotoxicity induced by these drugs involves metabolic activation by CYP2C9. Benzbromarone is metabolized via 6-hydroxybenzbromarone to the catechol by CYP2C9, followed by the oxidization of the catechol to a reactive *ortho*-quinone metabolite (McDonald and Rettie, 2007). Tienilic acid is metabolized via the sulfoxide to 5-hydroxytienilic acid by CYP2C9. This sulfoxide can form a covalent bond with CYP2C9 or other proteins. In rat, administration of tienilic acid in combination with the glutathione biosynthesis inhibitor, buthionine sulfoximine (BSO), induced a marked elevation of the serum alanine aminotransferase (ALT) level, but no increase in the serum ALT activity was observed in the presence of the P450 inhibitor, 1-aminobenzotoriazole (Nishiya et al., 2008). Thus, the mechanisms for the metabolic activation of these drugs have been well examined. However, to our knowledge, cell-based assays for assessment of the metabolic activations of these drugs have not been performed. The results obtained in our cell-based assay system were in agreement with several reports that CYP2C9 is involved in the metabolic activations of benzbromarone and tienilic acid. However, there have been no reports of the involvement of CYP2C9 in the cytotoxicity of losartan. It has been reported that losartan could form protein or glutathione adducts by incubation with human liver microsomes and/or human hepatocytes, suggesting the metabolic activation of losartan (Gan et al., 2009; Usui et al., 2009). The present study demonstrated for the first time that CYP2C9 was responsible for the metabolic activation of losartan. The concentrations at which the metabolic activation of losartan was observed were much higher than those in plasma in clinical practice. To predict the involvement of CYP2C9 in losartan-induced toxicity, the combination of our established cell-based assay with other studies is needed.

Sartans have generally been used as safe drugs in clinical practice, but there have been various reports of losartan-induced hepatotoxicity, which is categorized as hepatocellular injury (Tabak et al., 2002; Chang and Schiano, 2007). In some case reports, a rechallenge to losartan after ALT normalization caused hepatotoxicities again (Bosch, 1997; Tabak et al., 2002). However, the contribution of immunological factors to losartan-induced hepatotoxicity was unknown. Losartan is metabolized to the carboxylic acid metabolite E3174, which is pharmacologically more active than the parent compound, via the aldehyde metabolite E3179, which is an intermediate in the oxidation of losartan. These biotransformations are catalyzed by CYP2C9 and CYP3A4. In addition to this pathway, the monohydroxylation of the butyl side chain is also catalyzed by CYP2C9 (Stearns et al., 1995). The viability of HepG2 cells was not decreased by treatment of E3179 and E3174 (Supplemental Fig. 1), suggesting that they may not show cytotoxicity. In this study, two CYP2C9-specific semicarbazide adducts of losartan (S1 and S2) were detected (Figs. 6 and 7). From the fragment ions of S1 and S2, it was suggested that S2 was produced via E3179, but S1 was not (Fig. 8). The cytotoxicity of losartan induced by CYP2C9 was attenuated by the treatment with semicarbazide (Supplemental Fig. 2). Therefore, the possible reactive metabolites from S1 and S2 might be involved in the cytotoxicity. Furthermore, no significant decreases in cell viabilities were observed by treatment with various sartans (irbesartan, valsartan, candesartan, olmesartan, telmisartan, and eprosartan) other than losartan. Taken together, these results suggested that the side chains or a chloro group besides the imidazole ring that is unique to losartan is important for the losartan-induced cytotoxicity mediated by CYP2C9.

The CYP2C9-induced cytotoxicities of benzbromarone, tienilic acid, and losartan were enhanced by Nrf2 knockdown, suggesting that the genes regulated by Nrf2 are associated with detoxification of their cytotoxicities. In our recent study, CYP3A4-induced cytotoxicities of several drugs such as acetaminophen and flutamide were sensitively detected by Nrf2 knockdown (H. Hosomi, T. Fukami, A. Iwamura, M. Nakajima, and T. Yokoi, manuscript submitted for publication). In addition, it was demonstrated that *nrf2*(−/−) mice are more vulnerable to acetaminophen-induced liver injury, due in part to lower cellular thiol levels and decreased expression of detoxification enzymes (Enomoto et al., 2001). Thus, Nrf2 is considered to play a quite important role in the detoxification of hepatotoxic drugs. Among the genes regulated by Nrf2, there are various genes involved in glutathione synthesis, such as the glutamate cysteine ligase catalytic subunit, the glutamate cysteine ligase regulatory subunit, and glutathione synthetase (Copple et al., 2008). Glutathione is an important intracellular peptide that detoxifies reactive metabolites by conjugation (Lu, 1999). In fact, reactive *ortho*-quinone metabolites of benzbromarone generated by CYP2C9 can be trapped with glutathione (McDonald and Rettie, 2007). In addition, the presence of glutathione markedly decreased the level of covalent binding of tienilic acid to microsomal proteins (Bonierbale et al., 1999). From these backgrounds, we considered whether the cytotoxicity of losartan could be clearly observed in a cytotoxicity assay with HepG2 cells transfected with siRNA for γ-glutamylcysteine synthetase heavy chain or treated with BSO instead of being transfected with siNrf2. However, no significant decreases in cell viabilities were observed by either transfection of siRNA for γ-glutamylcysteine synthetase heavy chain or treatment with BSO (data not shown). These results suggested that glutathione conjugation was not required for the detoxification of losartan-induced cytotoxicity but that other detoxification enzymes regulated by Nrf2 would be involved. Therefore, semicarbazide was used as a trapping agent for the reactive metabolites of losartan in this study. Semicarbazide is a hard nucleophile, which will preferentially react with hard electrophiles, such as aldehydes (Chauret et al., 1995). Indeed, the cytotoxicity of losartan induced by CYP2C9 was attenuated by treatment with semicarbazide (Supplemental Fig. 2). Thus, it is conceivable that reactive metabolites trapped by semicarbazide are involved in the CYP2C9-induced cytotoxicity of losartan.

In the present study, CYP2C9-mediated metabolic activation was not observed with flutamide, fluvastatin, terbinafine, valproic acid, and zolpidem, which are suspected to be associated with hepatotoxicity (Karsenti et al., 1999; Thole et al., 2004; Chang and Schiano, 2007). Flutamide is hydrolyzed to 4-nitro-3-(trifluoromethyl)phenylamine (FLU-1), which is further metabolized to *N*-hydroxy FLU-1, which can cause hepatotoxicity in rat (Ohbuchi et al., 2009). The N-hydroxylation of FLU-1 is catalyzed by CYP2C9 as well as by CYP3A4 (Goda et al., 2006). In this study, flutamide-induced cytotoxicity could not be detected. One possibility is that the intracellular concentration of FLU-1 was low because of the low flutamide hydrolase activity in HepG2 cells, although it was not measured. Terbinafine is known to be metabolized by a wide range of P450 enzymes including CYP2C9, primarily through N-demethylation, deamination, and hydroxylation (Vickers et al., 1999). Among its metabolites, 7,7-dimethylhept-2-ene-4-ynal was considered to play a role in the pathogenesis of hepatotoxicity (Iverson and Uetrecht, 2001), but this

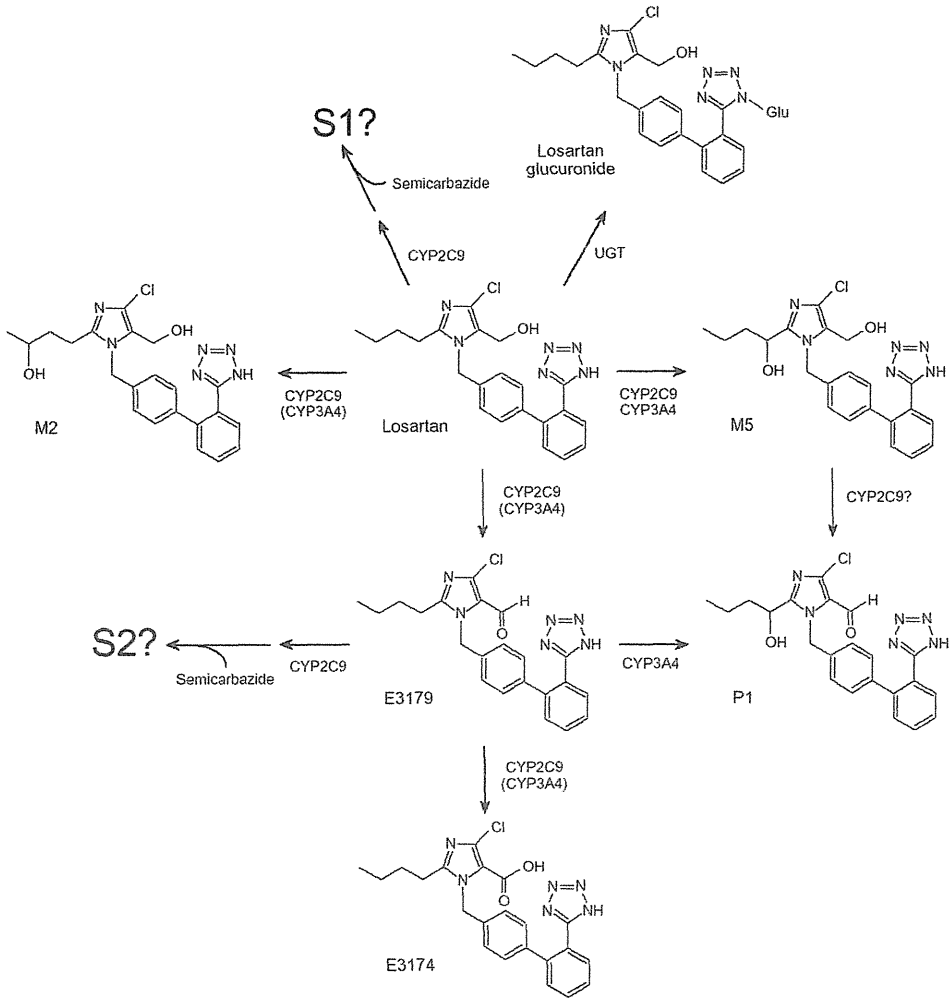

FIG. 8. Proposed metabolic pathways of losartan. UGT, UDP-glucuronosyltransferase.

metabolite is generated by CYP3A4, not by CYP2C9. That is why the cell viability was not affected by treatment with terbinafine in AdCYP2C9-infected cells. For the hepatotoxicity caused by valproic acid, the involvement of its reactive metabolites such as 4-ene-valproic acid and 2,4-diene-valproic acid was suggested (Baillie, 1988; Kassahun et al., 1991; Tang et al., 1995). CYP2C9 played a role in the formation of 4-ene-valproic acid (Sadeque et al., 1997), but no involvement of CYP2C9 in the cytotoxicity of valproic acid was observed in this study. It was reported that valproic acid produced a high level of covalent binding in rat liver after oral administration, although it did not bind to microsomal protein in vitro (Leone et al., 2007). Other factors as well as CYP2C9 might be responsible for the hepatotoxicity of valproic acid. The cytotoxicities of fluvastatin and zolpidem induced by CYP2C9 were not detected in the present study. Until now, the mechanisms of their cytotoxicities have been unknown. The present study suggested low involvement of CYP2C9 in their cytotoxicities, although it is responsible for the metabolism of these drugs (Fischer et al., 1999; Von Moltke et al., 1999).

In conclusion, we constructed a highly sensitive cell-based assay system to evaluate CYP2C9-mediated cytotoxicity and found for the first time that CYP2C9 is involved in the metabolic activation of losartan. This cell-based assay system would be useful in evaluating drug-induced cytotoxicity caused by human CYP2C9.

Acknowledgments

We thank Toru Usui and Dr. Takanori Hashizume (Pharmacokinetics Research Laboratories, Dainippon Sumitomo Pharma Co., Ltd., Osaka, Japan) for technical assistance with LC-MS/MS and LCMS-IT-TOF analyses and Brent Bell for reviewing the manuscript.

Authorship Contributions

Participated in research design: Iwamura, Fukami, Nakajima, and Yokoi.
Conducted experiments: Iwamura and Hosomi.
Contributed new reagents or analytic tools: Iwamura and Hosomi.
Performed data analysis: Iwamura and Fukami.
Wrote or contributed to the writing of the manuscript: Iwamura, Fukami, and Yokoi.

References

Baillie TA (1988) Metabolic activation of valproic acid and drug-mediated hepatotoxicity. Role of the terminal olefin, 2-*n*-propyl-4-pentenoic acid. *Chem Res Toxicol* **1:**195–199.
Bonierbale E, Valadon P, Pons C, Desfosses B, Dansette PM, and Mansuy D (1999) Opposite behaviors of reactive metabolites of tienilic acid and its isomer toward liver proteins: use of specific anti-tienilic acid-protein adduct antibodies and the possible relationship with different hepatotoxic effects of the two compounds. *Chem Res Toxicol* **12:**286–296.
Bosch X (1997) Losartan-induced hepatotoxicity. *JAMA* **278:**1572.
Chang CY and Schiano TD (2007) Review article: drug hepatotoxicity. *Aliment Pharmacol Ther* **25:**1135–1151.
Chauret N, Nicoll-Griffith D, Friesen R, Li C, Trimble L, Dubé D, Fortin R, Girard Y, and Yergey J (1995) Microsomal metabolism of the 5-lipoxygenase inhibitors L-746,530 and L-739,010 to reactive intermediates that covalently bind to protein: the role of the 6,8-dioxabicyclo[3.2.1]octanyl moiety. *Drug Metab Dispos* **23:**1325–1334.
Copple IM, Goldring CE, Kitteringham NR, and Park BK (2008) The Nrf2-Keap1 defence pathway: role in protection against drug-induced toxicity. *Toxicology* **246:**24–33.
Edwards RJ, Adams DA, Watts PS, Davies DS, and Boobis AR (1998) Development of a comprehensive panel of antibodies against the major xenobiotic metabolising forms of cytochrome P450 in humans. *Biochem Pharmacol* **56:**377–387.
Enomoto A, Itoh K, Nagayoshi E, Haruta J, Kimura T, O'Connor T, Harada T, and Yamamoto M (2001) High sensitivity of Nrf2 knockout mice to acetaminophen hepatotoxicity associated with decreased expression of ARE-regulated drug metabolizing enzymes and antioxidant genes. *Toxicol Sci* **59:**169–177.

DMD DRUG METABOLISM AND DISPOSITION aspet
Downloaded from dmd.aspetjournals.org at Kanazawa Univ Yakugakubu Lib on May 2, 2011

Fischer V, Johanson L, Heitz F, Tullman R, Graham E, Baldeck JP, and Robinson WT (1999) The 3-hydroxy-3-methylglutaryl coenzyme A reductase inhibitor fluvastatin: effect on human cytochrome P-450 and implications for metabolic drug interactions. *Drug Metab Dispos* **27:**410–416.

Gan J, Ruan Q, He B, Zhu M, Shyu WC, and Humphreys WG (2009) In vitro screening of 50 highly prescribed drugs for thiol adduct formation—comparison of potential for drug-induced toxicity and extent of adduct formation. *Chem Res Toxicol* **22:**690–698.

Goda R, Nagai D, Akiyama Y, Nishikawa K, Ikemoto I, Aizawa Y, Nagata K, and Yamazoe Y (2006) Detection of a new *N*-oxidized metabolite of flutamide, *N*-[4-nitro-3-(trifluoromethyl)-phenyl]hydroxylamine, in human liver microsomes and urine of prostate cancer patients. *Drug Metab Dispos* **34:**828–835.

Greer ML, Barber J, Eakins J, and Kenna JG (2010) Cell based approaches for evaluation of drug-induced liver injury. *Toxicology* **268:**125–131.

Guengerich FP (2008) Cytochrome P450 and chemical toxicology. *Chem Res Toxicol* **21:**70–83.

Hewitt NJ and Hewitt P (2004) Phase I and II enzyme characterization of two sources of HepG2 cell lines. *Xenobiotica* **34:**243–256.

Hosomi H, Akai S, Minami K, Yoshikawa Y, Fukami T, Nakajima M, and Yokoi T (2010) An in vitro drug-induced hepatotoxicity screening system using CYP3A4-expressing and γ-glutamylcysteine synthetase knockdown cells. *Toxicol In Vitro* **24:**1032–1038.

Iverson SL and Uetrecht JP (2001) Identification of a reactive metabolite of terbinafine: insights into terbinafine-induced hepatotoxicity. *Chem Res Toxicol* **14:**175–181.

Karsenti D, Blanc P, Bacq Y, and Metman EH (1999) Hepatotoxicity associated with zolpidem treatment. *BMJ* **318:**1179.

Kassahun K, Farrell K, and Abbott F (1991) Identification and characterization of the glutathione and *N*-acetylcysteine conjugates of (*E*)-2-propyl-2,4-pentadienoic acid, a toxic metabolite of valproic acid, in rats and humans. *Drug Metab Dispos* **19:**525–535.

Koenigs LL, Peter RM, Hunter AP, Haining RL, Rettie AE, Friedberg T, Pritchard MP, Shou M, Rushmore TH, and Trager WF (1999) Electrospray ionization mass spectrometric analysis of intact cytochrome P450: identification of tienilic acid adducts to P450 2C9. *Biochemistry* **38:**2312–2319.

Lee WM (2003) Drug-induced hepatotoxicity. *N Engl J Med* **349:**474–485.

Leone AM, Kao LM, McMillian MK, Nie AY, Parker JB, Kelley MF, Usuki E, Parkinson A, Lord PG, and Johnson MD (2007) Evaluation of felbamate and other antiepileptic drug toxicity potential based on hepatic protein covalent binding and gene expression. *Chem Res Toxicol* **20:**600–608.

Li AP (2002) A review of the common properties of drugs with idiosyncratic hepatotoxicity and the "multiple determinant hypothesis" for the manifestation of idiosyncratic drug toxicity. *Chem Biol Interact* **142:**7–23.

Lu SC (1999) Regulation of hepatic glutathione synthesis: current concepts and controversies. *FASEB J* **13:**1169–1183.

McDonald MG and Rettie AE (2007) Sequential metabolism and bioactivation of the hepatotoxin benzbromarone: formation of glutathione adducts from a catechol intermediate. *Chem Res Toxicol* **20:**1833–1842.

Mizuno K, Katoh M, Okumura H, Nakagawa N, Negishi T, Hashizume T, Nakajima M, and Yokoi T (2009) Metabolic activation of benzodiazepines by CYP3A4. *Drug Metab Dispos* **37:**345–351.

Nishiya T, Kato M, Suzuki T, Maru C, Kataoka H, Hattori C, Mori K, Jindo T, Tanaka Y, and Manabe S (2008) Involvement of cytochrome P450-mediated metabolism in tienilic acid hepatotoxicity in rats. *Toxicol Lett* **183:**81–89.

O'Brien PJ, Irwin W, Diaz D, Howard-Cofield E, Krejsa CM, Slaughter MR, Gao B, Kaludercic N, Angeline A, Bernardi P, et al. (2006) High concordance of drug-induced human hepatotoxicity with in vitro cytotoxicity measured in a novel cell-based model using high content screening. *Arch Toxicol* **80:**580–604.

Ohbuchi M, Miyata M, Nagai D, Shimada M, Yoshinari K, and Yamazoe Y (2009) Role of enzymatic *N*-hydroxylation and reduction in flutamide metabolite-induced liver toxicity. *Drug Metab Dispos* **37:**97–105.

Park BK, Kitteringham NR, Maggs JL, Pirmohamed M, and Williams DP (2005) The role of metabolic activation in drug-induced hepatotoxicity. *Annu Rev Pharmacol Toxicol* **45:**177–202.

Rodríguez-Antona C, Donato MT, Boobis A, Edwards RJ, Watts PS, Castell JV, and Gómez-Lechón MJ (2002) Cytochrome P450 expression in human hepatocytes and hepatoma cell lines: molecular mechanisms that determine lower expression in cultured cells. *Xenobiotica* **32:**505–520.

Sadeque AJ, Fisher MB, Korzekwa KR, Gonzalez FJ, and Rettie AE (1997) Human CYP2C9 and CYP2A6 mediate formation of the hepatotoxin 4-ene-valproic acid. *J Pharmacol Exp Ther* **283:**698–703.

Stearns RA, Chakravarty PK, Chen R, and Chiu SH (1995) Biotransformation of losartan to its active carboxylic acid metabolite in human liver microsomes. Role of cytochrome P4502C and 3A subfamily members. *Drug Metab Dispos* **23:**207–215.

Tabak F, Mert A, Ozaras R, Biyikli M, Ozturk R, Ozbay G, Senturk H, and Aktuglu Y (2002) Losartan-induced hepatic injury. *J Clin Gastroenterol* **34:**585–586.

Tang W, Borel AG, Fujimiya T, and Abbott FS (1995) Fluorinated analogues as mechanistic probes in valproic acid hepatotoxicity: hepatic microvesicular steatosis and glutathione status. *Chem Res Toxicol* **8:**671–682.

Thole Z, Manso G, Salgueiro E, Revuelta P, and Hidalgo A (2004) Hepatotoxicity induced by antiandrogens: a review of the literature. *Urol Int* **73:**289–295.

Usui T, Mise M, Hashizume T, Yabuki M, and Komuro S (2009) Evaluation of the potential for drug-induced liver injury based on in vitro covalent binding to human liver proteins. *Drug Metab Dispos* **37:**2383–2392.

Vickers AE, Sinclair JR, Zollinger M, Heitz F, Glänzel U, Johanson L, and Fischer V (1999) Multiple cytochrome P-450s involved in the metabolism of terbinafine suggest a limited potential for drug-drug interactions. *Drug Metab Dispos* **27:**1029–1038.

Vignati L, Turlizzi E, Monaci S, Grossi P, Kanter R, and Monshouwer M (2005) An in vitro approach to detect metabolite toxicity due to CYP3A4-dependent bioactivation of xenobiotics. *Toxicology* **216:**154–167.

Von Moltke LL, Greenblatt DJ, Granda BW, Duan SX, Grassi JM, Venkatakrishnan K, Harmatz JS, and Shader RI (1999) Zolpidem metabolism *in vitro*: responsible cytochromes, chemical inhibitors, and *in vivo* correlations. *Br J Clin Pharmacol* **48:**89–97.

Yoshikawa Y, Hosomi H, Fukami T, Nakajima M, and Yokoi T (2009) Establishment of knockdown of superoxide dismutase 2 and expression of CYP3A4 cell system to evaluate drug-induced cytotoxicity. *Toxicol In Vitro* **23:**1179–1187.

Address correspondence to: Dr. Tsuyoshi Yokoi, Drug Metabolism and Toxicology, Faculty of Pharmaceutical Sciences, Kanazawa University, Kakuma-machi, Kanazawa 920-1192, Japan. E-mail: tyokoi@kenroku.kanazawa-u.ac.jp

DMD DRUG METABOLISM AND DISPOSITION aspet

Toxicology Letters 204 (2011) 17–24

Contents lists available at ScienceDirect

Toxicology Letters

journal homepage: www.elsevier.com/locate/toxlet

Estradiol and progesterone modulate halothane-induced liver injury in mice

Yasuyuki Toyoda[a], Taishi Miyashita[a], Shinya Endo[a], Koichi Tsuneyama[b], Tatsuki Fukami[a], Miki Nakajima[a], Tsuyoshi Yokoi[a,*]

[a] Drug Metabolism and Toxicology, Faculty of Pharmaceutical Sciences, Kanazawa University, Kakuma-machi, Kanazawa 920-1192, Japan
[b] Department of Diagnostic Pathology, Graduate School of Medicine and Pharmaceutical Science for Research, University of Toyama, Sugitani 930-0194, Toyama, Japan

ARTICLE INFO

Article history:
Received 27 January 2011
Received in revised form 29 March 2011
Accepted 30 March 2011
Available online 8 April 2011

Keywords:
Drug-induced liver injury
Halothane
Estradiol
Progesterone

ABSTRACT

Drug-induced liver injury (DILI) is one of the major problems in drug development and clinical drug therapy. In general, it is believed that women exhibit worse outcomes from DILI than men. It is known that halothane (HAL), an inhaled anesthetic, rarely induces severe liver injury. The risk factors for severe HAL-induced liver injury (HILI) are female sex, genetics and adult age. To investigate the underlying mechanism by which women are more susceptible to HILI, we focused on two major female sex hormones, estradiol (E2) and progesterone (Prog). In this study, we first found that pretreatment of mice with E2 attenuated HILI, whereas pretreatment with Prog exacerbated HILI. E2 and Prog had no effects on the degree of metabolic activation, the ratio of GSH/GSSG or oxidative stress in the liver. We observed higher numbers of neutrophils infiltrated into the liver and increased hepatic mRNA levels of proinflammatory cytokines, tumor necrosis factor (TNF) α, interleukin (IL)-1β and IL-6 and chemokines, CXCL1 and CXCL2 by pretreatment with Prog, whereas E2 pretreatment resulted in the opposite effects. These results suggest that E2 and Prog play a critical role in HILI via immune-related responses and female sex hormone balance might represent a risk factor for HILI.

© 2011 Elsevier Ireland Ltd. All rights reserved.

1. Introduction

The occurrence of drug-induced liver injury (DILI) can be a major problem in all phases of clinical drug development. In most cases, the mechanisms of hepatotoxicity are unknown, but it is likely to arise from complex interactions among drugs, genetic, age, gender, disease and environmental factors (Chalasani and Björnsson, 2010; Li, 2002). In general, women are more susceptible to DILI than men. Seventy-eight percent of DILI cases occur in women, and a significantly greater number of women show hepatocellular DILI than men (Ostapowicz et al., 2002; De Valle et al., 2006; Björnsson and Olsson, 2005). In contrast, some reports described that there was no significant gender difference in the incident rates of DILI (Lucena et al., 2009; Andrade et al., 2005). However, it was also reported that patients with severe DILI who underwent liver transplantation in the US were more frequently women (76%) and that nearly 90% of patients with fluminant liver injury from DILI were women. Thus, women appear to be at greater risk of developing severe DILI (Lucena et al., 2009; Andrade et al., 2005; Russo et al., 2004), but it is not clear why women exhibit the worst outcomes in DILI.

Women elicit more vigorous cellular and humoral immune reactions, and suffer in greater numbers from autoimmune disease than men (Ansar et al., 1985; Ostensen, 1999). There is also evidence that the immune system is regulated by the circulating levels of sex steroid hormones, estradiol (E2), progesterone (Prog), and testosterone (Grossman, 1985). It was also reported that E2 inhibits proinflammatory cytokine production by murine peritoneal macrophages and mononuclear cells in vitro, whereas Prog may counteract this effect of E2 (Huang et al., 2008; Yuan et al., 2008). However, there has been little information concerning the involvement of female sex hormones in DILI.

Halothane (HAL) is an inhaled anesthetic that causes asymptomatic increases of plasma transaminases in approximately 20% of patients and severe liver injury in a small percentage of patients (Ray and Drummond, 1991). Risk factors for severe halothane-induced liver injury (HILI) are female sex, adult age, genetics, and multiple halothane exposures (Inman and Mushin, 1974; Cousins et al., 1989). HAL is metabolized to trifluoroacetyl (TFA)-chloride by cytochrome P450 (CYP) 2E1 and covalent binding to proteins and lipids. It has been suggested that TFA-adduct or halothane-modified macromolecules may be an initiating event for an immune response (Bourdi et al., 2001; Njoku et al., 1997; Gut et al., 1993). Recent studies indicate the mechanism of HILI involves immune responses such as neutrophils, IL-17 and natural killer cells (You et al., 2006; Kobayashi et al., 2009; Cheng et al., 2010).

Recently, a new mouse model of HILI was established and gender differences in the degree of HILI were suggested (You et al.,

* Corresponding author. Tel.: +81 76 234 4407; fax: +81 76 234 4407.
E-mail address: tyokoi@kenroku.kanazawa-u.ac.jp (T. Yokoi).

0378-4274/$ – see front matter © 2011 Elsevier Ireland Ltd. All rights reserved.
doi:10.1016/j.toxlet.2011.03.031

2006). In this study, we investigated whether two major female sex hormones, E2 and Prog, play a functional role in HILI.

2. Materials and methods

2.1. Materials

HAL was purchased from Takeda (Osaka, Japan) and isoflurane (Iso) was from Abott Japan (Tokyo, Japan). 17β-Estradiol (E2) and Prog were from Sigma–Aldrich (St. Louis, MO). ICI182,780 (ICI) was from TOCRIS bioscience (Ellisville, MO) and RU486 (RU) was from Tokyo Kasei (Tokyo, Japan). Rabbit polyclonal antibody against myeloperoxidase (MPO) was from DAKO (Carpinteria, CA). All primers were commercially synthesized at Hokkaido System Sciences (Sapporo, Japan). All other chemicals were of the highest grade commercially available.

2.2. Mice and HAL-administration

Female BALB/cCrSlc mice (8 weeks old, 18–21 g) were obtained from SLC Japan (Hamamatsu, Japan). Animals were housed in a controlled environment (temperature 25 ± 1 °C, humidity 50 ± 10%, and 12-h light/12-h dark cycle) in the institutional animal facility with access to food and water *ad libitum*. Animals were acclimatized before use for the experiments (Sugaya et al., 2000). E2 and Prog pretreatment methods were modified from those of a previous report that the serum hormone levels were almost the same or slightly higher than those during late pregnancy in rodent, although the mice used in the present study were not ovariectomized since we intend to perform the present studies under the autologus condition and to mimic the condition of late pregnancy. Mice were pretreated with E2 (0.3 μg/mouse, s.c.) or Prog (0.3 mg/mouse, s.c.) for 7 days followed by HAL administration (15 or 30 mmol/kg, dissolved in olive oil 2 mL/20 g of body weight, *i.p.*) 1.5 h after the last E2 or Prog treatment. Mice were pretreated with the receptor antagonist, ICI (Estrogen receptor (ER) antagonist, 50 μg/mouse, *s.c.*) or RU (Progesterone receptor (PR) antagonist, 50 μg/mouse, s.c.) 0.5 h before the E2 or Prog treatment, respectively. In the Isoflurane (Iso) administration experiment, Iso was administered instead of HAL. Mice were sacrificed and the plasma and the liver were collected 3, 6 and 24 h after the HAL administration. The liver was fixed in buffered neutral 10% formalin and used for immunohistochemical staining. The degree of liver injury was assessed by hematoxylin–eosin (H&E) staining and the plasma aspartate aminotransferase (AST) and alanine aminotransferase (ALT) levels were determined using Fuji Dri-Chem 4000V (Fuji Film Med. Co., Tokyo, Japan). The neutrophil infiltration was assessed by immunostaining for MPO as previously described (Kumada et al., 2004). Animal maintenance and treatment were conducted in accordance with the National Institutes of Health Guide for Animal Care and Use Committee of Kanazawa University, Japan.

2.3. Measurement of plasma E2, Prog and IL-17 levels

Plasma E2 and Prog were measured by enzyme immunoassay (EIA) using Estradiol-17β (serum/plasma) EIA kit and Progesterone EIA kit from Assay Designs Inc. (Ann Arbor, MI) according to the manufacturer's instructions. The plasma IL-17 level was measured by ELISA using a Ready-SET-GO! Mouse Interleukin-17A (IL-17A) kit from eBioscience (San Diego, CA) according to the manufacturer's instructions.

2.4. Immunoblot analysis

SDS-polyacrylamide gel electrophoresis and immunoblot analysis were perfomed. Mouse liver homogenates (30 μg) were separated on 10% polyacrylamide gels and electrotransferred onto polyvinylidene difluoride membrane, Immobion-P (Millipore Corporation, Billerica, MA). The membranes were probed with goat anti-rat Cyp2e1 (1:10,000, Daiichi Pure Chemicals, Tokyo, Japan), anti-TFA antisera (1:1000, kindly provided by Dr. Lance Pohl, National Institutes of Health, Bethesda, MD) and rabbit anti-human glyceraldehyde-3-phoshate dehydrogenase (GAPDH) polyclonal antibodies (1:100, IMAGENEX, San Diego, CA) and the corresponding fluorescent dye-conjugated second antibody (1:5000) and an Odyssey Infrared Imaging System (LI-COR Biosciences, Lincoln, NE) were used for detection. The relative expression level was quantified using ImageQuant TL Image Analysis software (GE Healthcare, Buckinghamshire, UK).

2.5. Glutathione assay

Mouse liver was homogenized with a glass homogenizer on ice-cold 5% sulfosalicylic acid and centrifuged at 8000 × *g* at 4 °C for 10 min. Total GSH and GSSG concentration in the supernant were measured as described previously (Tietze, 1969; Griffith, 1980). GSH was calculated from the difference between the total GSH and GSSG concentration.

Table 1
Sequence of primers used for real-time RT-PCR analyses in this study.

Target	Primer	Sequence
TNFα	FP	5′-TGT CTC AGC CTC TTC TCA TTC C-3′
	RP	5′-TGA GGG TCT GGG CCA TAG AAC-3′
IL-1β	FP	5′-GTT GAC GGA CCC CAA AAG AT-3′
	RP	5′-CAC ACA CCA GCA GGT TAT CA-3′
IL-6	FP	5′-CCA TAG CTA CCT GGA GTA CA-3′
	RP	5′-GGA AAT TGG GGT AGG AAG GA-3′
CXCL1	FP	5′-GAT TCA CCT CAA GAA CAT CCA GAG-3′
	RP	5′-GAA GCC AGC GTT CAC CAG AC-3′
CXCL2	FP	5′-AAG TTT GCC TTG ACC CTG AAG-3′
	RP	5′-ATC AGG TAC GAT CCA GGC TTC-3′
ICAM-1	FP	5′-CAA GGA GAT CAC ATT CAC GG-3′
	RP	5′-CTT CCA GGG AGC AAA ACA AC -3′

FP, forward primer; RP, reverse primer.

2.6. Protein carbonyl content measurement

The protein carbonyl was measured in whole liver homogenate using a Protein Carbonyl kit (Cell biolabs, Tokyo, Japan). The assay was performed according to the manufacturer's instructions.

2.7. Real-time reverse transcription (RT)-PCR analysis

RNA from mouse liver was isolated using RNAiso according to the manufacturer's instructions. Tumor necrosis factor α (TNFα), Interleukin (IL)-1β, IL-6, Chemokine (C-X-C motif) ligand 1, 2 (CXCL1, CXCL2), intercellular adhesion molecule-1 (ICAM-1), and Gapdh were quantified by real-time RT-PCR. The primer sequences used in this study are shown in Table 1. The reverse transcription process and real-time RT-PCR were performed as described previously (Kobayashi et al., 2009).

2.8. Statistical analysis

Data are presented as mean ± SD. Comparison of 2 groups was made with an unpaired, two-tailed Student's *t*-test. Comparison of multiple groups was made with ANOVA followed by Dunnett or Tukey test. A value of $P < 0.05$ was considered statistically significant.

3. Results

3.1. The effects of E2 and Prog on halothane-induced liver injury

To investigate the role of the female sex hormones on HILI, female BALB/c mice pretreated with E2 or Prog were administered with HAL at a dose of 30 or 15 mmol/kg, respectively. The plasma E2 levels were 87.72 ± 15.98 pg/mL in mice 24 h after the last E2 pretreatment and 42.39 ± 18.85 pg/mL in mice pretreated with vehicle. The plasma Prog levels was 80.43 ± 33.25 ng/mL in mice 24 h after the last Prog pretreatment and 29.24 ± 14.77 ng/mL in mice pretreated with vehicle. Plasma transaminase levels were not changed 3 and 6 h after the HAL administration (data not shown). In addition, E2 or Prog pretreatment only did not affect the plasma transaminase levels 3 and 6 h after the HAL administration (data not shown). At 24 h after the HAL administration, E2 pretreatment significantly decreased the plasma transaminase levels compared with HAL (30 mg/kg) alone and Prog pretreatment caused a remarkable increase of the plasma transaminase levels compared to HAL (15 mg/kg) alone. These effects were significantly inhibited by pretreatment with ICI (ER antagonist) or RU (PR antagonist) in E2 or Prog pretreated groups, respectively (Fig. 1A). Histopathological changes demonstrated that E2 pretreatment decreased hepatocyte degeneration and damage lesions, which were enhanced by Prog pretreatment. In addition, immunohistochemical analyses with anti-MPO antibody demonstrated that E2 pretreatment decreased the numbers of MPO-positive cells infiltrated in liver at 24 h after HAL administration, whereas Prog pretreatment increased (Fig. 1B). From these results, pretreatment of mice with E2 attenuated HILI, whereas pretreatment of mice with Prog exacerbated HILI and these effects were likely mediated via each hormone receptor. Iso,

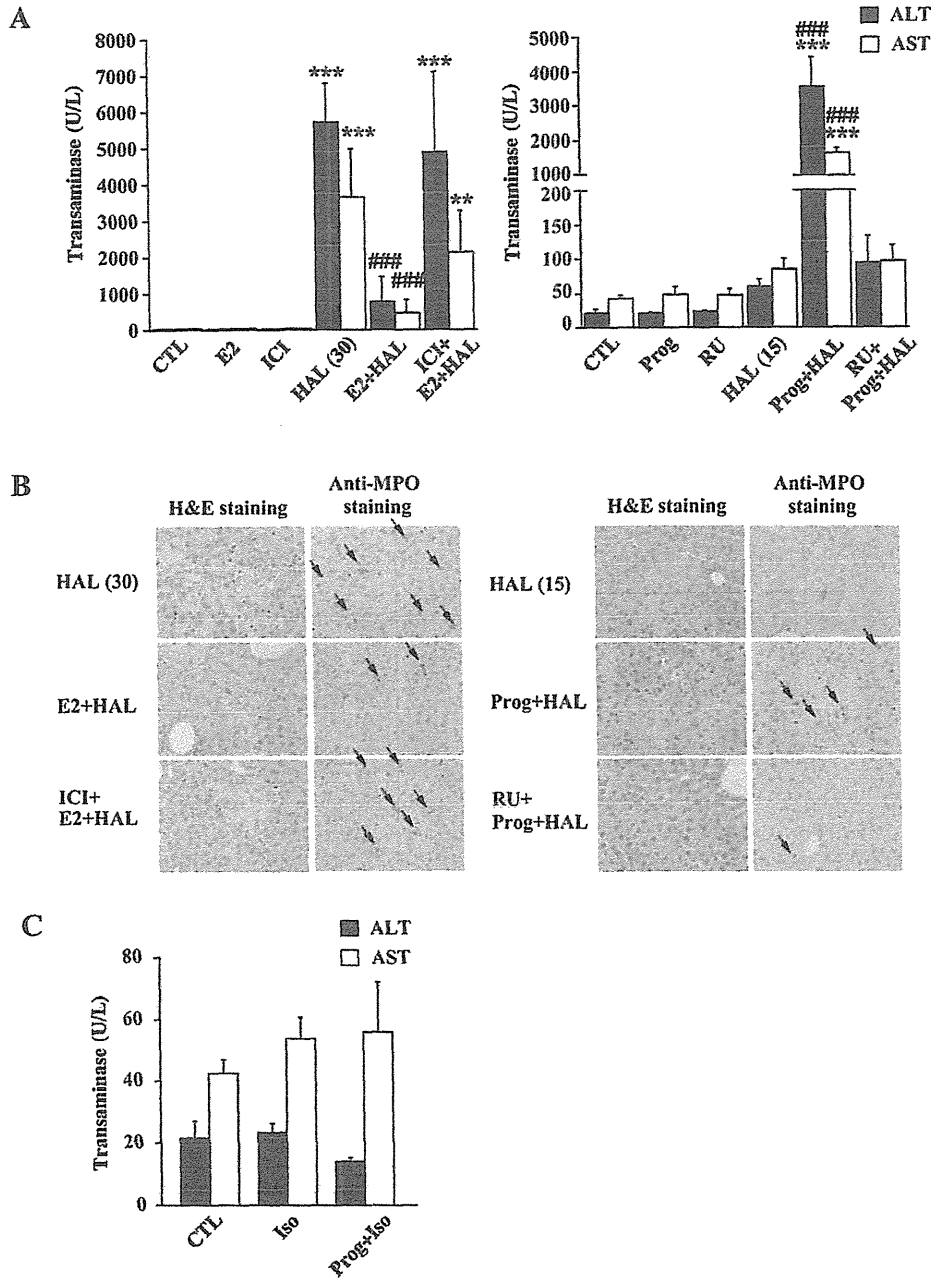

Fig. 1. Effects of E2 or Prog administration in HAL-induced liver injury. Mice (female, 8-week old) were pretreated with E2 (0.3 μg/mouse, *s.c.*), Prog (0.3 mg/mouse, *s.c.*) or vehicle (CTL: olive oil) for 7 days followed by HAL administration (15 or 30 mmol/kg, *i.p.*) or Iso administration (15 mmol/kg, *i.p.*) 1.5 h after the last treatment of E2 or Prog. In experiments using antagonist, mice were treated with ICI (50 μg/mouse, s.c.) or RU (50 μg/mouse, s.c.) 0.5 h prior to the treatment with E2 or Prog, respectively for 7 days. Twenty-four hours after the HAL or Iso administration, serum samples were collected for assessment of the transaminase levels (A and C). Liver tissue sections were stained with H&E or immunostained with anti-MPO antibody (B). Arrows indicate MPO-positive cells. The data are mean ± SD of 4–5 mice. $^{**}P < 0.01$ and $^{***}P < 0.001$, campared with CTL. $^{\#\#\#}P < 0.001$, compared with only HAL-administered mice.

structurally and pharmacologically similar to HAL, is less hepatotoxic than HAL (Njoku et al., 1997). In female BALB/c mice, the transaminase levels were not increased at doses up to 30 mmol/kg of Iso (data not shown). In addition, Prog pretreatment showed no effects on the serum transaminase levels at 24 h after the Iso administration (Fig. 1C).

3.2. E2 and Prog had no effect on the metabolic activation of halothane or on the oxidative stress

HAL is metabolized by CYP2E1 to reactive metabolites, trifluoroacetyl radicals, which bind a number of hepatic proteins in human, rats and mice (Bourdi et al., 2001; Njoku et al., 1997; Gut et al., 1993). To investigate whether the pretreatment with E2 or Prog affected the metabolic activation of HAL, immunoblotting was performed using anti-TFA polyclonal antibody and goat anti rat Cyp2e1 antibody. No difference was found in either the profiles or levels of TFA–protein adducts formed in the liver of mice pretreated with E2 or Prog 24 h after the HAL administration (Fig. 2A). In addition, the expression levels of Cyp2e1 protein in E2- or Prog-pretreated mouse liver also showed no changes (Fig. 2B). GSH plays a protective role against HILI in guinea pig (Lind et al., 1992). To investigate whether GSH and oxidative stress were modulated by pretreatment with E2 or Prog, the ratio of GSH/GSSG and

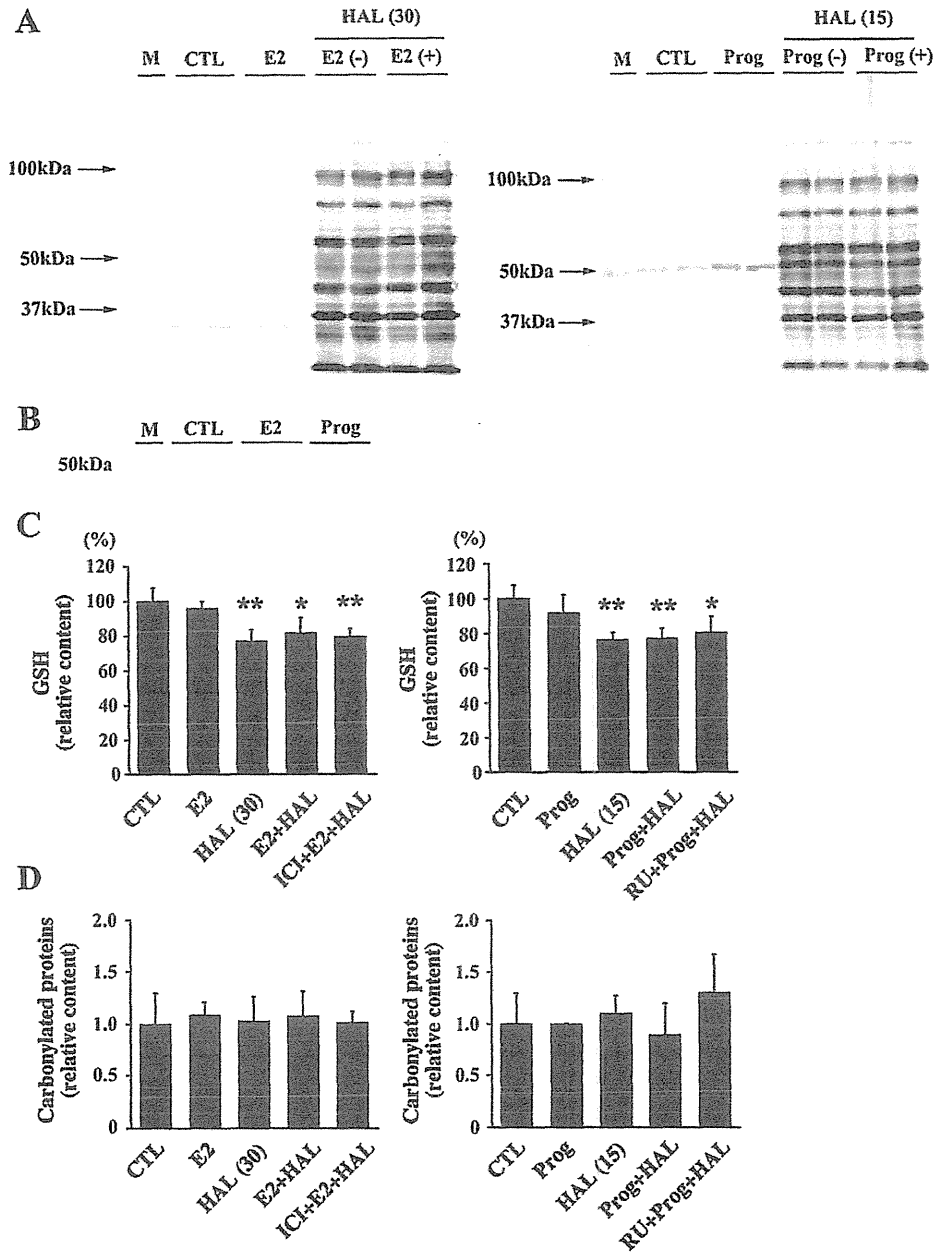

Fig. 2. Effects of E2 or Prog administration on the degree of metabolic activation, the ratio of GSH/GSSG and oxidative stress in the liver in HAL-induced liver injury. Experimental conditions for animal treatments were the same as those in Fig. 1. Twenty-four hours after the HAL administration, liver samples were collected. Immunoblot of TFA–protein adducts (A), Cyp2e1 protein expression (B) and Gapdh, a lording control, were performed using whole liver homogenate. Each lane shows an individual mouse (30 μg/lane). The ratio of GSH/GSSG (C) and carbonylated proteins (D) in whole liver homogenate were measured. The data are mean ± SD of 4 mice. $^{*}P < 0.05$ and $^{**}P < 0.01$, campared with CTL. M: molecular weight marker.

carbonylated proteins, a biomarker of oxidative stress, in the liver were measured. The ratio of GSH/GSSG of the HAL-administered groups were significantly decreased to 50–70% of the control group, but there was no effect on the ratio of GSH/GSSG in E2- or Prog-pretreated mouse liver (Fig. 2C). In addition, the levels of carbonylated proteins were also not altered (Fig. 2D). These results indicated that E2 and Prog had no effect on the metabolic activation of HAL or on the oxidative stress.

3.3. *E2 and Prog modulated the immune responses in halothane-induced liver injury*

In many cases, inflammation reactions and immune-related cells play a crucial role in DILI. In HILI, proinflammatory cytokines and neutrophils play important roles in the propagation of tissue damage (You et al., 2006; Kobayashi et al., 2009; Cheng et al., 2010). To investigate whether E2 or Prog pretreatment affect the production of inflammatory cytokines (TNFα, IL-1β and IL-6), potent neutrophil chemotactic chemokines, CXCL1 and CXCL2, and ICAM-1, which are important in the transendothelial migration of neutrophils, hepatic mRNA was measured. E2 pretreatment alone did not affect the production of proinflammatory cytokines, chemokines and ICAM-1 (Fig. 3). The expression of TNFα, IL-1β and IL-6 were significantly increased compared with CTL at indicated time after the HAL administration (Fig. 3A). Similarly, CXCL1 and ICAM-1 were significantly increased compared with CTL at 3 and 6 h after HAL administration and CXCL2 was markedly increased at 24 h after the HAL administration (Fig. 3B). Moreover, E2 pretreat-

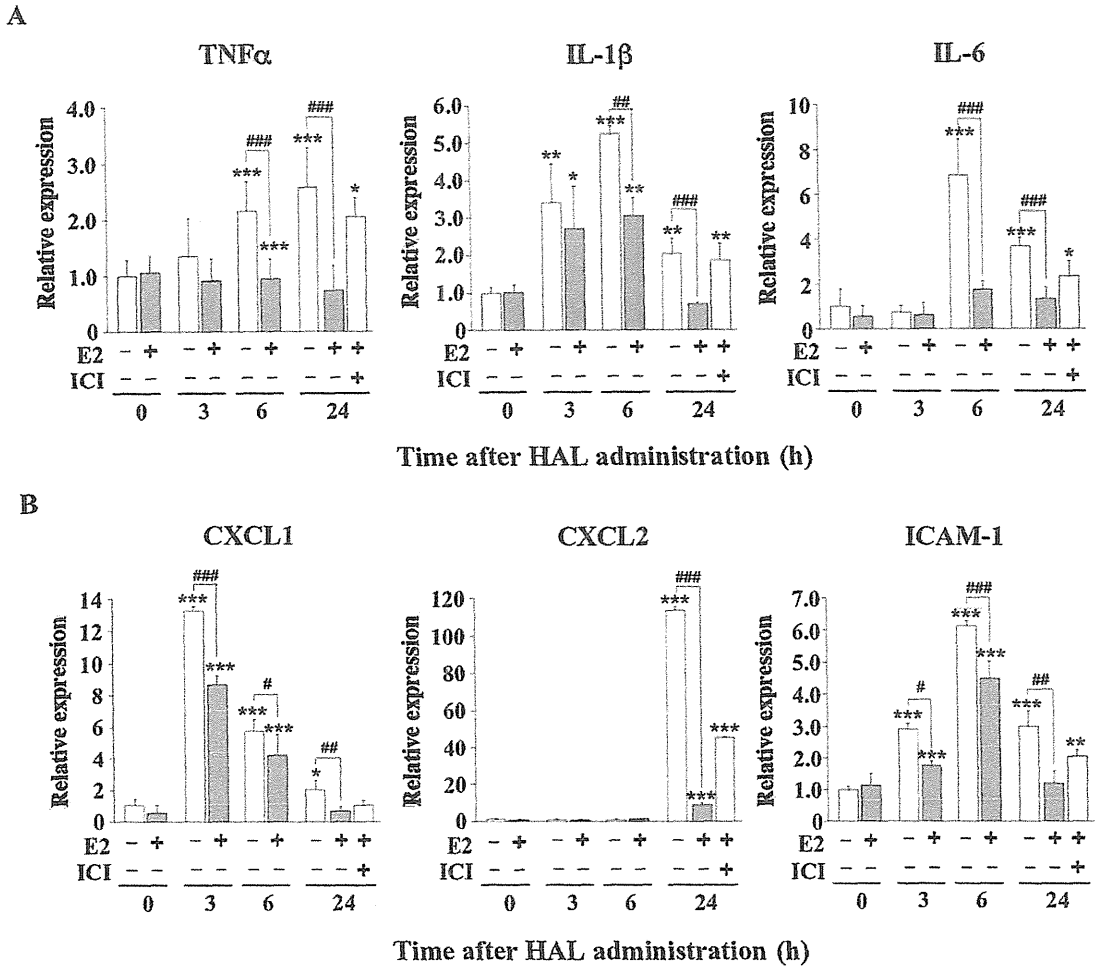

Fig. 3. Time-dependent changes of immune responses by E2 pretreatment in HAL-administered mice. Experimental conditions for animal treatments were the same as those in Fig. 1. Relative expression of hepatic mRNA was measured for proinflammatory cytokines (A) and chemokines and ICAM-1 related to neutrophil infiltration (B) in the E2-pretreated mouse liver 0, 3, 6 and 24 h after the HAL administration. Expression of hepatic mRNA was normalized to Gapdh mRNA. The data are mean ± SD of 4–5 mice. $^{*}P<0.05$, $^{**}P<0.01$ and $^{***}P<0.001$, campared with CTL. $^{\#}P<0.05$, $^{\#\#}P<0.01$ and $^{\#\#\#}P<0.001$, compared with only HAL-administered mice.

ment significantly decreased inflammatory mediators compared with HAL alone. These effects of E2 were blocked by ICI administration (Fig. 3).

Interestingly, Prog pretreatment alone significantly upregulated CXCL1, whereas proinflammatory cytokines, CXCL2 and ICAM-1 did not change (Fig. 4). Prog pretreatment significantly increased the expression of TNFα, IL-1β and IL-6 at indicated time after the HAL administration (Fig. 4A). Similarly, Prog pretreatment significantly increased CXCL1, CXCL2 and ICAM-1 at indicated time after the HAL administration (Fig. 4B). These effects of Prog were blocked by RU administration (Fig. 4). These results suggested that E2 and Prog played a crucial role in HILI by modulating the hepatic inflammation.

3.4. E2 and Prog modulated the production of IL-17 in halothane-induced liver injury

We previously demonstrated that IL-17 is involved in HILI (Kobayashi et al., 2009). To investigate whether E2 or Prog pretreatment affect the production of IL-17, plasma IL-17 level was measured. The IL-17 level was significantly increased only 24 h after the HAL (30 mmol/kg) administration, but not HAL (15 mmol/kg) administration (Fig. 5). E2 or Prog pretreatment alone did not affect the IL-17 levels. As with the expression of inflammatory mediators (Figs. 3 and 4), E2 pretreatment significantly decreased and Prog pretreatment significantly increased the plasma IL-17 levels (Fig. 5). These effects of E2 or Prog were blocked by ICI or RU administration, respectively (Fig. 5).

4. Discussion

Generally, women exhibit worse outcomes from liver injury than men (Lucena et al., 2009; Andrade et al., 2005; Russo et al., 2004). In this study, we focused on two major female sex hormones, E2 and Prog. The circulating levels of E2 and Prog fluctuate as a result of the reproductive phase and pregnancy in women (Wood et al., 2007; Barkley et al., 1979). E2 reduces the severity of various types of liver injuries such as ischemia-reperfusion, trauma-hemorrhage and acetaminophen, but there is little information about the role of Prog in liver injury (Yokoyama et al., 2005; Chandrasekaran et al., 2011; Shimizu et al., 2008). It has been reported that immune-based diseases may have exacerbations during the reproductive phase (Ansar et al., 1985; Ostensen, 1999). Since the activation of immune cells plays an important role in HILI (You et al., 2006; Kobayashi et al., 2009; Cheng et al., 2010), we hypothesized that female sex hormones would affect HILI.

To investigate whether two female sex hormones affect HILI, mice were pretreated with E2 or Prog for 7 days followed by HAL administration. In this study, the E2 and Prog concentrations were

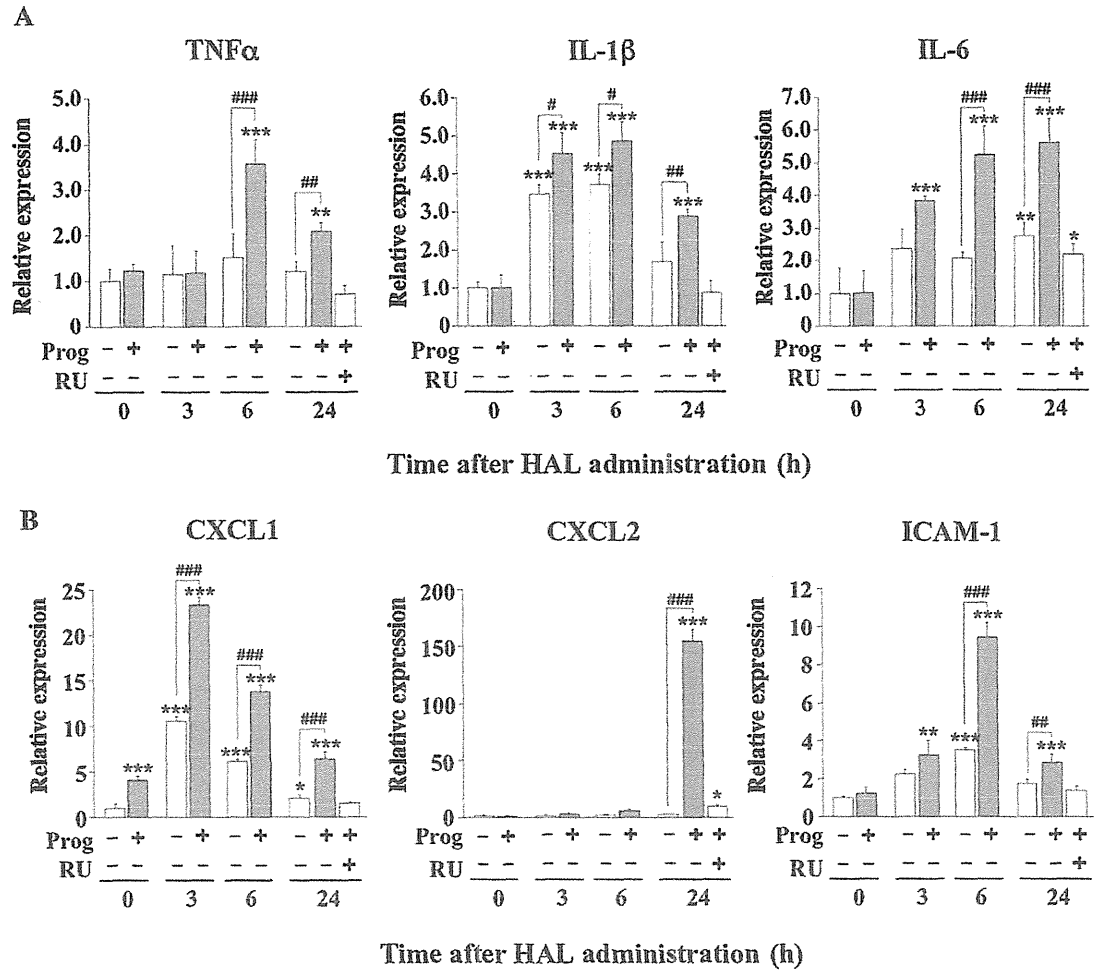

Fig. 4. Time-dependent changes of immune responses by Prog pretreatment in HAL-administered mice. Experimental conditions for animal treatments were the same as those in Fig. 1. Relative expression of hepatic mRNA was measured for proinflammatory cytokines (A) and chemokines and ICAM-1 related to neutrophil infiltration (B) in the Prog-pretreated mouse liver 0, 3, 6 and 24 h after the HAL administration. Expression of hepatic mRNA was normalized to Gapdh mRNA. The data are mean ± SD of 4–5 mice. $^{*}P<0.05$, $^{**}P<0.01$ and $^{***}P<0.001$, compared with CTL. $^{\#}P<0.05$, $^{\#\#}P<0.01$ and $^{\#\#\#}P<0.001$, compared with only HAL-administered mice.

higher in E2 or Prog-pretreated mice than the vehicle treated mice. The plasma E2 levels were 87.72 ± 15.98 pg/mL in mice pretreated with E2 and the plasma Prog levels were 80.43 ± 33.25 ng/mL in mice pretreated with Prog. In general, E2 and Prog secretion increased to maximum during the late pregnancy, plasma E2 level of 60–120 pg/mL and plasma Prog level of 60–120 ng/mL, respectively (Barkley et al., 1979). Therefore, mice pretreated with E2 or Prog in the present study was almost the same as those during

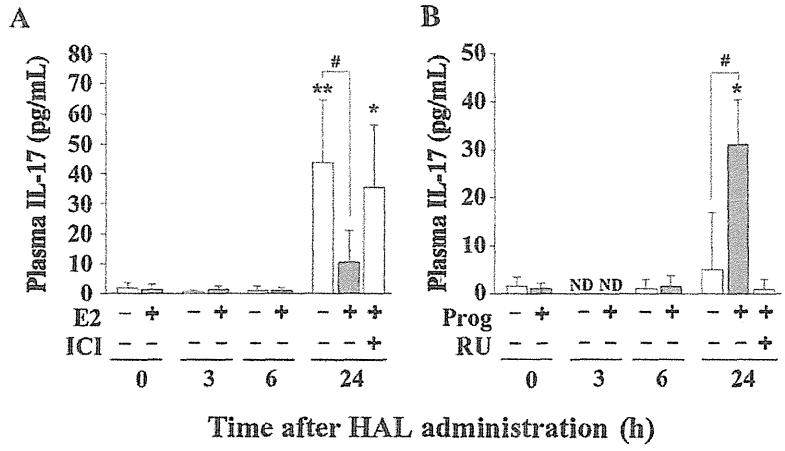

Fig. 5. Time-dependent changes of plasma IL-17 by E2 or Prog pretreatment in HAL-administered mice. Experimental conditions for animal treatments were the same as those in Fig. 1. Plasma IL-17 level was measured in mice pretreated with E2 or Prog 0, 3, 6 and 24 h after the HAL administration (E2; 30 mmol/kg, Prog; 15 mmol/kg). The data are mean ± SD of 4–5 mice. $^{*}P<0.05$ and $^{**}P<0.01$, compared with CTL. $^{\#}P<0.05$, compared with only HAL-administered mice. ND: not detected.

late pregnancy. The transaminase levels and hepatic damage in HILI were attenuated by E2 pretreatment and exacerbated by Prog pretreatment at 24 h but not at 3 and 6 h after the HAL administration (Fig. 1). Neutrophils play a crucial role in the pathology of HILI (You et al., 2006; Kobayashi et al., 2009; Cheng et al., 2010). In this study, MPO-positive cells that infiltrated in the liver were decreased by E2 pretreatment and increased by Prog pretreatment suggesting that E2 and Prog may modulate the degree of HILI via neutrophils. Iso is widely used clinically and shows less hepatotoxicity than HAL (Njoku et al., 1997). No changes in transaminases were observed in mice administered Iso alone. Moreover, Prog pretreatment did not affect the transaminase levels in Iso-administered mice (Fig. 1C). These results indicated that Prog exacerbates the severity of liver injury rather than causing the liver injury. These results may relate to the fact that women exhibit worse outcomes in DILI (Lucena et al., 2009; Andrade et al., 2005; Russo et al., 2004). Moreover, these results indicated that the balance of E2 and Prog changed as a result of the reproductive phase and pregnancy in women affect the severity of DILI.

It has been suggested that TFA–protein adducts caused mild hepatotoxicity and initiated immune reactions (Bourdi et al., 2001; Njoku et al., 1997; Gut et al., 1993). E2 and Prog pretreatment did not affect TFA–protein adduct formation and Cyp2e1 expression (Fig. 2A and B). It was also reported that GSH-depleted guinea pigs exhibited a significant enhancement of HILI (Lind et al., 1992). Recently, it was reported that E2 attenuated APAP-induced liver injury by inhibiting oxidative stress (Chandrasekaran et al., 2011). However, in the present study E2 and Prog pretreatment had no effect on the depletion of the ratio of GSH/GSSG and protein carbonyl contents after HAL administration (Fig. 2C and D). These results indicated that the effects of E2 or Prog may not be involved in the metabolic activation of HAL and oxidative stress. Thus, it is suggested that E2 and Prog are related to another pathway in the pathogenesis of HILI.

Activated immune cells contribute to enhancing liver injury by releasing proinflammatory cytokines and chemokines to further hepatic inflammation, which determines the extent of liver injury (Kaplowitz, 2005; Adams et al., 2010). It has been demonstrated that proinflammatory cytokines, such as TNFα, IL-1β and IL-6, were decreased by E2 pretreatment and enhanced by Prog pretreatment in HILI. In addition, CXC chemokines (CXCL1 and CXCL2) and ICAM-1, which play an important role in neutrophil infiltration, were decreased by E2 pretreatment and enhanced by Prog pretreatment (Figs. 3 and 4). It is reported that transaminase levels achieved peak at 24 h after the HAL administration (You et al., 2006; Kobayashi et al., 2009). Although transaminase levels were not increased at earlier time point (3 or 6 h), the expression levels of TNFα, IL-1β, IL-6, CXCL1 and ICAM-1 were modulated by E2 and Prog pretreatment at earlier time point after HAL administration (Figs. 3 and 4). These results suggested that E2 and Prog affect the severity of HILI by modulating the production of proinflammatory cytokines and chemokines. CXC chemokines and ICAM-1 mRNA expression levels were correlated with neutrophil infiltration and accumulation in the histopathology of HILI (Figs. 1, 3 and 4). CXC chemokines are considered to attract predominantly neutrophils to the liver under stress conditions and the neutrophils undergo adhesion to hepatocytes via hepatocyte ICAM-1 (Ramaiah and Jaeschke, 2007). Furthermore, the roles of neutrophils have been demonstrated in a variety of liver diseases (Ramaiah and Jaeschke, 2007; Li et al., 2004; Frink et al., 2007). It is suggested that these mediators are related to neutrophil infiltration into the liver in HILI.

Interestingly, CXCL1 is increased by Prog pretreatment. CXCL1 not only mediates neutrophil infiltration, but also causes hepatotoxicity effects itself, which lead to massive liver necrosis in preinjured liver (Ramaiah and Jaeschke, 2007; Li et al., 2004; Frink et al., 2007; Stefanovic et al., 2005). In addition, previous studies have demonstrated the important role of CXCL1 in liver injury such as trauma-hemorrhage, endotoxemia and CCl_4-induced liver injury (Shimizu et al., 2008; Ramaiah and Jaeschke, 2007; Li et al., 2004; Frink et al., 2007; Stefanovic et al., 2005). It was also reported that recombinant CXCL1 had no effect in normal liver (Stefanovic et al., 2005). In accordance with these findings, Prog pretreatment had no hepatotoxic effect in normal mice and exacerbated liver injury by HAL administration but not by Iso administration (Fig. 1). We previously reported that IL-17 is involved in HILI (Kobayashi et al., 2009). In this study, changes of IL-17 were correlated with transaminases after HAL administration. E2 or Prog pretreatment alone do not affect the levels of IL-17 (Figs. 1 and 5). Although IL-17 does not initiate an immune response, IL-17 is able to amplify immune response of the early stage (Maione et al., 2009). IL-17-induced immune response was significantly reduced in mice treated with anti-CXCL1 antibody (Maione et al., 2009). Therefore, CXCL1 might play an important role in the progression of HILI by Prog pretreatment in the early stage of immune response.

Previous studies reported that E2 and Prog modulate proinflammatory cytokine production by murine peritoneal macrophages and human mononuclear cells in vitro. These reports also demonstrated that the hormonal effects were mediated by hormonal receptors (Huang et al., 2008; Yuan et al., 2008). In addition, E2 decreased the production of CXCL1 from KC via ER following trauma-hemorrhage (Shimizu et al., 2008). KCs act as the major source of proinflammatory cytokines (TNFα, IL-1β and IL-6) and CXC chemokines under severe stress and various liver injuries (Kaplowitz, 2005; Adams et al., 2010; Laskin, 1990; Mosher et al., 2001). The effects of E2 and Prog on HILI and immune responses were blocked by ICI or RU administration, respectively (Figs. 1, 3 and 4) indicating that the effects of E2 and Prog on HILI could be mediated via ER and PR, respectively. Thus, it might be thought that E2 and Prog affect immune cells responding to E2 and Prog via each receptor, such as monocytes or macrophages, which might result in modulation the immune reaction in HILI.

In conclusions, this study indicated that E2 attenuated and Prog exacerbated the severity of HILI via immune-related reactions. This is the first report that E2 and Prog modulated the severity of HILI. It is also indicated that the E2/Prog hormone balance might represent a risk factor for HILI and that female sex hormones might have a role in one of the mechanism of sex differences in HILI.

Funding

Health and Labor Sciences Research Grants from the Ministry of Health, Labor and Welfare of Japan (H20-BIO-G001).

Conflict of interest

None of the authors has any conflicts of interest related to this manuscript.

Acknowledgement

We thank Mr. Brent Bell for reviewing the manuscript.

References

Adams, D.H., Ju, C., Ramaiah, S.K., Uetrecht, J., Jaeschke, H., 2010. Mechanisms of immune-mediated liver injury. Toxicol. Sci. 115, 307–321.

Andrade, R.J., Lucena, M.I., Fernández, M.C., Pelaez, G., Pachkoria, K., Garciá-Ruiz, E., Garciá-Muñoz, B., González-Grande, R., Pizarro, A., Durán, J.A., Jiménez, M., Rodrigo, L., Romero-Gomez, M., Navarro, J.M., Planas, R., Costa, J., Borras, A., Soler, A., Salmerón, J., Martin-Vivaldi, R., Spanish Group for the Study of Drug-Induced Liver Disease, 2005. Drug-induced liver injury: an analysis of 461 incidences submitted to the Spanish registry over a 10-year period. Gastroenterology 129, 512–521.

Ansar, A.S., Penhale, W.J., Talal, N., 1985. Sex hormones, immune responses, and autoimmune diseases. Mechanisms of sex hormone action. Am. J. Pathol. 121, 531–551.
Barkley, M.S., Geschwind, I.I., Bradford, G.E., 1979. The gestational pattern of estradiol, testosterone and progesterone secretion in selected strains of mice. Biol. Reprod. 20, 733–738.
Björnsson, E., Olsson, R., 2005. Outcome and prognostic markers in severe drug-induced liver disease. Hepatology 42, 481–489.
Bourdi, M., Amouzadeh, H.R., Rushmore, T.H., Martin, J.L., Pohl, L.R., 2001. Halothane-induced liver injury in outbred guinea pigs: role of trifluoracetylated protein adducts in animal susceptibility. Chem. Res. Toxicol. 14, 362–370.
Chalasani, N., Björnsson, E., 2010. Risk factors for idiosyncratic drug-induced liver injury. Gastroenterogy 138, 2246–2259.
Chandrasekaran, V.R., Periasamy, S., Liu, L.L., Liu, M.Y., 2011. 17β-Estradiol protects against acetaminophen-overdose-induced acute oxidative hepatic damage and increases the survival rate in mice. Steroids 76, 118–124.
Cheng, L., You, Q., Yin, J., Holt, M.P., Ju, C., 2010. Involvement of natural killer T cells in halothane-induced liver injury in mice. Biochem. Phamacol. 80, 255–261.
Cousins, M.J., Plummer, J.L., Hall, P.D., 1989. Risk factors for halothane hepatitis. Aust. N. Z. J. Surg. 59, 5–14.
De Valle, M.B., Av Klinteberg, V., Alem, N., Olsson, R., Björnsson, E., 2006. Drug-induced liver injury in a Swedish University hospital out-patient hepatology clinic. Aliment. Pharmacol. Ther. 24, 1187–1195.
Frink, M., Hsieh, Y.C., Hsieh, C.H., Pape, H.C., Choudhry, M.A., Schwacha, M.G., Chaudry, I.H., 2007. Keratiocyte-derived chemokine plays a critical role in the induction of systemic inflammation and tissue damage after trauma-hemorrhage. Shock 28, 576–581.
Griffith, O.W., 1980. Determination of glutathione and glutathione disulfide using glutathione reductase and 2-vinylpyridine. Anal. Biochem. 106, 207–212.
Grossman, C.J., 1985. Interactions between the gonadal steroids and the immune system. Science 227, 257–261.
Gut, J., Christen, U., Huwyler, J., 1993. Mechanisms of halothane toxicity: novel insights. Pharmacol. Ther. 58, 133–155.
Huang, H., He, J., Yin, Y., Aoyagi, E., Takenaka, H., Itagaki, T., Sannomiya, K., Tamaki, K., Harada, N., Shono, M., Shimizu, I., Takayama, T., 2008. Opposing effects of estradiol and progesterone on the oxidative stress-induced production of chemokine and proinflammatory cytokines in murine peritoneal macrophages. J. Med. Invest. 55, 133–141.
Inman, W.H., Mushin, W.W., 1974. Jaundice after repeated exposure to halothane: analysis of reports to the committee on safety of medicines. Br. Med. J. 1, 5–10.
Kaplowitz, N., 2005. Idiosyncratic drug hepatotoxicity. Nat. Rev. Drug Discov. 4, 489–499.
Kobayashi, E., Kobayashi, M., Tsuneyama, K., Fukami, T., Nakajima, M., Yokoi, T., 2009. Halothane-induced liver injury is mediated by interleukin-17 in mice. Toxicol. Sci. 111, 302–310.
Kumada, T., Tsuneyama, K., Hatta, H., Ishizawa, S., Takano, Y., 2004. Improved 1-h rapid immunostaining method using intermittent microwave irradiation: practicability based on 5 years application in Toyama Medical and pharmaceutical University Hospital. Mod. Pathol. 17, 1141–1149.
Laskin, D.L., 1990. Nonparenchymal cells and hepatotoxicity. Semin. Liver Dis. 10, 293–304.
Li, A.P., 2002. A review of the common properties of drugs with idiosyncratic hepatotoxicity and the "multiple determinant hypothesis" for the manifestation of idiosyncratic drug toxicity. Chem. Biol. Interact. 142, 7–23.
Li, X., Klintman, D., Liu, Q., Sato, T., Jeppsson, B., Thorlacius, H., 2004. Critical role of CXC chemokines in endotoxemic liver injury in mice. J. Leukoc. Biol. 75, 443–452.
Lind, R.C., Gandolfi, A.J., Hall, P.M., 1992. Glutathione depletion enhances subanesthetic halothane hepatotoxicity in guinea pigs. Anesthesiology 77, 721–727.
Lucena, M.I., Andrade, R.J., Kaplowitz, N., García-Cortes, M., Fernández, M.C., Romero-Gomez, M., Bruguera, M., Hallal, H., Robels-Diaz, M., Rodriguez-González, J.F., Navarro, J.M., Salmeron, J., Martinez-Odriozola, P., Pérez-Alvarez, R., Borraz, Y., Hidalgo, R., Spanish Group for the Study of Drug-induced Liver Disease, 2009. Phenotypic characterization of idiosyncratic drug-induced liver injury: the influence of age and sex. Hepatology 49, 2001–2009.
Maione, F., Paschalidis, N., Mascolo, N., Dufton, N., Perretti, M., D'Acquisto, F., 2009. Interleukin 17 sustains rather than induces inflammation. Biochem. Pharmacol. 77, 878–887.
Mosher, B., Dean, R., Harkema, J., Remick, D., Palma, J., Crockett, E., 2001. Inhibition of kupffer cells reduced CXC chemokine production and liver injury. J. Surg. Res. 99, 201–210.
Njoku, D., Laster, M.J., Gong, D.H., Eger, E.I.2nd., Reed, G.F., Martin, J.L., 1997. Biotransformation of halothane, enflurane, isoflurane, and desflurane to trifluoroacetylated liver proteins: association between protein acylation and hepatic injury. Anesth. Analg. 84, 173–178.
Ostapowicz, G., Fontana, R.J., Schiødt, F.V., Larson, A., Davern, T.J., Han, S.H., McCashland, T.M., Shakil, A.O., Hay, J.E., Hynan, L., Crippin, J.S., Blei, A.T., Samuel, G., Reisch, J., Lee, W.M., U.S. Acute Liver Filure Study Group, 2002. Results of a prospective study of acute liver failure at 17 tertiary care centers in the United States. Ann. Intern. Med. 137, 947–954.
Ostensen, M., 1999. Sex hormones and pregnancy in rheumatoid arthritis and systemic lupus erythematosus. Ann. N. Y. Acad. Sci. 876, 131–143.
Ramaiah, S.K., Jaeschke, H., 2007. Role of neutrophils in the pathogenesis of acute inflammatory liver injury. Toxicol. Pathol. 35, 757–766.
Ray, D.C., Drummond, G.B., 1991. Halothane hepatitis. Br. J. Anaethsiol. 67, 84–99.
Russo, M.W., Galanko, J.A., Shrestha, R., Fried, M.W., Watkins, P., 2004. Liver transplantation for acute liver failure from drug induced liver injury in the United States. Liver Transpl. 10, 1018–1023.
Shimizu, T., Suzuki, T., Yu, H., Yokoyama, Y., Choudhry, M.A., Bland, K.I., Chaudry, I.H., 2008. The role of estrogen receptor subtypes on hepatic neutrophil accumulation following trauma-hemorrhage: direct modulation of CINC-1 production by kupffer cells. Cytokine 43, 88–92.
Stefanovic, L., Brenner, D.A., Stefanovic, B., 2005. Direct hepatotoxic effect of KC chemokaine in the liver without infiltration of neutrophils. Exp. Biol. Med. 230, 573–586.
Sugaya, A., Sugiyama, T., Yanase, S., Shen, X.X., Minoura, H., Toyoda, N., 2000. Expression of glucose transporter 4 mRNA in adipose tissue and skeletal muscle of ovariectomized rats treated with sex steroid hormones. Life Sci. 66, 641–648.
Tietze, F., 1969. Enzymatic method for quantitative determination of nanogram amounts of total and oxidized glutathione: applications to mammalian blood and other tissues. Anal. Biochem. 27, 502–522.
Wood, G.A., Fata, J.E., Watson, K.L., Khokha, R., 2007. Circulating hormones and estrous stage predict cellular and stromal remodeling in murine uterus. Reproduction 133, 1035–1044.
You, Q., Cheng, L., Reilly, T.P., Wegmann, D., Ju, C., 2006. Role of neutrophils in a mouse model of halothane-induced liver injury. Hepatology 44, 1421–1431.
Yuan, Y., Shimizu, I., Shen, M., Aoyagi, E., Takenaka, H., Itagaki, T., Urada, M., Sannomiya, K., Kohno, N., Shuno, M., Takayama, T., 2008. Effects of estradiol and progesterone on the proinflammatory cytokine production by mononuclear cells from patients with chronic hepatitis C. World J. Gastroenterol. 14, 2200–2207.
Yokoyama, Y., Nimura, Y., Nagio, M., Bland, K.I., Chaudry, I.H., 2005. Current understanding of gender dimorphism in hepatic pathophysiology. J. Surg. Res. 128, 147–156.

Supplemental Material can be found at:
http://dmd.aspetjournals.org/content/suppl/2011/04/21/dmd.111.038661.DC1.html

0090-9556/11/3907-1303–1310$25.00
DRUG METABOLISM AND DISPOSITION
Copyright © 2011 by The American Society for Pharmacology and Experimental Therapeutics
DMD 39:1303–1310, 2011

Vol. 39, No. 7
38661/3699032
Printed in U.S.A.

In Vitro Investigation of the Glutathione Transferase M1 and T1 Null Genotypes as Risk Factors for Troglitazone-Induced Liver Injury[S]

Toru Usui, Takanori Hashizume, Takashi Katsumata, Tsuyoshi Yokoi, and Setsuko Komuro

Pharmacokinetics Research Laboratories, Dainippon Sumitomo Pharma Co., Ltd., Osaka, Japan (T.U., T.H., T.K., S.K.); and Drug Metabolism and Toxicology, Faculty of Pharmaceutical Sciences, Kanazawa University, Kanazawa, Japan (T.U., T.Y.)

Received February 8, 2011; accepted April 21, 2011

ABSTRACT:

The double null mutation of glutathione transferase, GSTM1 and GSTT1, is reported to influence troglitazone-associated abnormal increases of alanine aminotransferase and aspartate aminotransferase. However, no nonclinical data with a bearing on the clinical outcomes and underlying mechanisms have hitherto been reported. To investigate whether deficiency in GSTM1 and/or GSTT1 is related to troglitazone hepatotoxicity in vitro, the covalent binding level (CBL) (an index of reactive metabolite formation) and cytotoxicity of troglitazone and rosiglitazone, another thiazolidinedione but with low hepatotoxicity, were examined using human liver samples phenotyped for cytochrome P450s and genotyped for GSTM1 and GSTT1. Despite addition of GSH, CBLs of troglitazone and rosiglitazone in human liver microsomes were correlated with CYP3A (or CYP2C8) and CYP2C8 activities, respectively. With addition of recombinant GSTM1, the microsomal CBLs of troglitazone and rosiglitazone decreased. However, the CBLs of troglitazone in GSTM1/GSTT1 wild-type hepatocytes were unexpectedly higher than those in null hepatocytes. Although this discrepancy has not been fully explained, the GSTM1 and GSTT1 null mutations increased the cytotoxicity of troglitazone, independent of CYP3A or CYP2C8 activities. Furthermore, a GSH adduct of troglitazone, M2, limited to GSTM1 wild-type hepatocytes was detected. Of clear interest, GSTM1 and/or GSTT1 null mutation-dependent cytotoxicity and higher exposure to the reactive metabolite trapped as M2 as for troglitazone were not observed for rosiglitazone. This result might at least partly explain the findings related to clinical hepatotoxicity, suggesting that measurement of GSH adducts or cytotoxicity using GSTM1- and GSTT1-genotyped hepatocytes might offer an important in vitro system to assist in better prediction of idiosyncratic hepatotoxicity.

Introduction

Troglitazone (Rezulin) (Fig. 1) was the first thiazolidinedione peroxisome proliferator-activated receptor γ agonist developed for the treatment of type II diabetes (Fujiwara et al., 1995; Sparano and Seaton, 1998). It was also the first in its class approved by the U.S. Food and Drug Administration for marketing in 1997 but was subsequently found to induce severe idiosyncratic hepatotoxicity in rare instances (Gitlin et al., 1998; Shibuya et al., 1998), which led to its withdrawal from the market in 2000. In the meantime, reports of usually milder and reversible hepatotoxicity have been documented very rarely with other thiazolidinediones, such as rosiglitazone (Avandia) (Fig. 1) and pioglitazone (Actos) (Isley, 2003). As a particularly interesting example for research on drug-induced liver injury (DILI), numerous researchers have investigated the mechanisms of troglitazone hepatotoxicity.

Although troglitazone hepatotoxicity was not predicted from tests in conventional experimental animals (Watanabe et al., 1999), some cellular events induced by troglitazone may have contributed to the clinically observed hepatotoxicity, for example, 1) reactive metabolite formation by oxidative cytochrome P450 (P450) 3A-mediated metabolism (Kassahun et al., 2001; Tettey et al., 2001; Yamamoto et al., 2002; He et al., 2004), 2) inhibition of the hepatic drug transporter, bile salt export pump or organic anion-transporting polypeptide by troglitazone sulfate (Funk et al., 2001a; Nozawa et al., 2004), 3) mitochondria-mediated toxicity by unchanged troglitazone (Masubuchi et al., 2006; Lim et al., 2008), 4) troglitazone-mediated apoptosis (Bae and Song, 2003; Shiau et al., 2005), and 5) down-regulation of proinflammatory cytokines in Kupffer cells (Sigrist et al., 2000). Although these nonclinical data cannot explain the idiosyncratic nature of troglitazone hepatotoxicity, high activity of drug-metabolizing enzymes (e.g., P450s) that form reactive metabolites or low activity of detoxification enzymes (e.g., glutathione transferases) (GSTs), which are responsible for scavenging reactive metabolites, are likely to be risk factors. In fact, with regard to this idiosyncrasy, there was a solitary and notable report indicating that the double mutation of GSTM1 and GSTT1 was associated with abnormally high levels of

Article, publication date, and citation information can be found at http://dmd.aspetjournals.org.
doi:10.1124/dmd.111.038661.
[S] The online version of this article (available at http://dmd.aspetjournals.org) contains supplemental material.

ABBREVIATIONS: DILI, drug-induced liver injury; P450, cytochrome P450; GST, glutathione transferase; ALT, alanine aminotransferase; AST, aspartate aminotransferase; CBL, covalent binding level; rh, recombinant human; HPLC, high-performance liquid chromatography; LC, liquid chromatography; MS/MS, tandem mass spectrometry; MRM, multiple reaction monitoring; UGT, UDP-glucuronosyltransferase; SULT, sulfotransferase; HLA, human leukocyte antigen.

Downloaded from dmd.aspetjournals.org at Kanazawa Univ Yakugakubu Lib on June 25, 2011

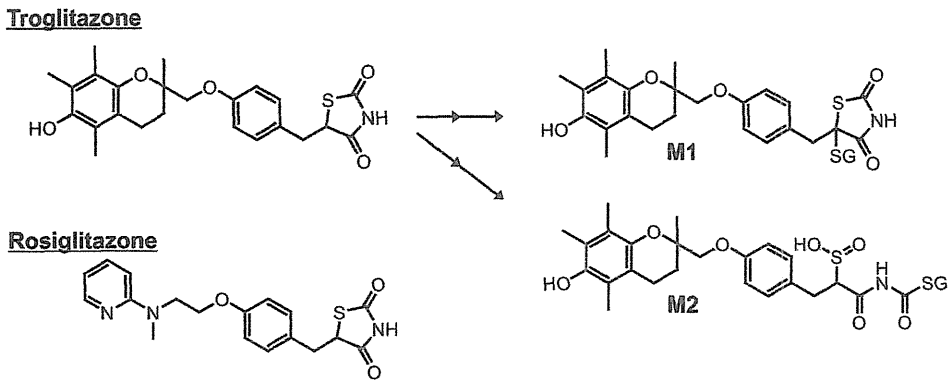

FIG. 1. Structures of troglitazone, rosiglitazone, and two postulated troglitazone GSH adducts. –SG, glutathione.

ALT and AST after administration of troglitazone on retrospective analysis using clinical samples (Watanabe et al., 2003). However, to our knowledge, no nonclinical data to link with the clinical outcomes and provide more detailed clues to mechanisms have hitherto been reported.

The purpose of the present study was to investigate whether GSTM1 and/or GSTT1 defects are involved in troglitazone hepatotoxicity in vitro. It is clear that metabolic activation of a drug to reactive metabolites and subsequent covalent binding to target macromolecules might be a necessary first step in the generation of idiosyncratic drug reactions in many cases (Walgren et al., 2005). We have already reported that covalent binding is one risk factor for DILI (Usui et al., 2009). Therefore, the covalent binding levels (CBLs) (an index of reactive metabolite formation) of troglitazone and rosiglitazone (as a negative control) were investigated using human in vitro liver samples with a diversity of P450 phenotypes or GST genotypes. Furthermore, cytotoxicity was also investigated to cast light on the idiosyncrasy of troglitazone hepatotoxicity.

Materials and Methods

Materials. [^{14}C]Troglitazone and [^{14}C]rosiglitazone were synthesized in-house. Unlabeled troglitazone and rosiglitazone were purchased from Toronto Research Chemicals Inc. (North York, ON, Canada). Pooled human liver microsomes (mixed-gender pool of 50 individuals) and 16 individual human liver microsome samples (Reaction Phenotyping Kit, version 7) were obtained from XenoTech, LLC (Lenexa, KS). Cryopreserved human hepatocytes were purchased from In Vitro Technologies, Inc. (Baltimore, MD) or XenoTech, LLC. The activities of major drug-metabolizing enzymes in microsomes and hepatocytes had been measured by the suppliers. Use of human samples in this study was approved by the ethics committee of the Drug Research Division, Dainippon Sumitomo Pharma Co., Ltd. (Osaka, Japan). Recombinant human (rh) GSTA1 and rhGSTM1, used in Fig. 2 (cytosol isolated from *Escherichia coli*-expressing human GSTA1 and GSTM1, respectively), and control cytosol (isolated from *E. coli* host strain) were purchased from Cypex Ltd. (Dundee, UK). rhGSTA1, rhGSTM1, and rhGSTP1, used in Supplemental Fig. 2, were purchased from PanVera Corp. (Madison, WI). To prepare the negative control of PanVera rhGST, rhGSTM1 was heat-inactivated at 90°C for 2 min. NADPH and reduced GSH were from Oriental Yeast Co., Ltd. (Tokyo, Japan), and Nacalai Tesque, Inc. (Kyoto, Japan), respectively. All other regents and solvents were of the highest grade commercially available.

Incubation Using Human Liver Microsomes. In microsomal assays, radiolabeled troglitazone and rosiglitazone (final concentration 10 μM) were incubated with 1 mg/ml pooled human liver microsomes or 16 individual human liver microsome samples phenotyped for P450 activities in the presence of 1 mM NADPH and 1 mM GSH at 37°C for 1 h in 500 μl of a reaction mixture consisting of 50 mM phosphate buffer (pH 7.4). rhGSTA1, rhGSTM1, rhGSTP1, or control cytosol (0.4 mg/ml) was added as required.

Genotyping for GSTM1 and GSTT1 Using Human Hepatocytes. GSTM1 and GSTT1 genotyping was performed by polymerase chain reaction amplification of genomic DNA as described previously (Arand et al., 1996). Genomic DNA was isolated from human hepatocytes using a DNeasy Blood and Tissue Kit (QIAGEN, Hilden, Germany).

Incubation Using Cryopreserved Human Hepatocytes for Measurement of CBL and Metabolite Analysis. Radiolabeled compounds (10 μM) were incubated with cryopreserved human hepatocytes (1 × 10^6 cells/ml) genotyped for GSTM1 and GSTT1 at 37°C for 8 h under an atmosphere of

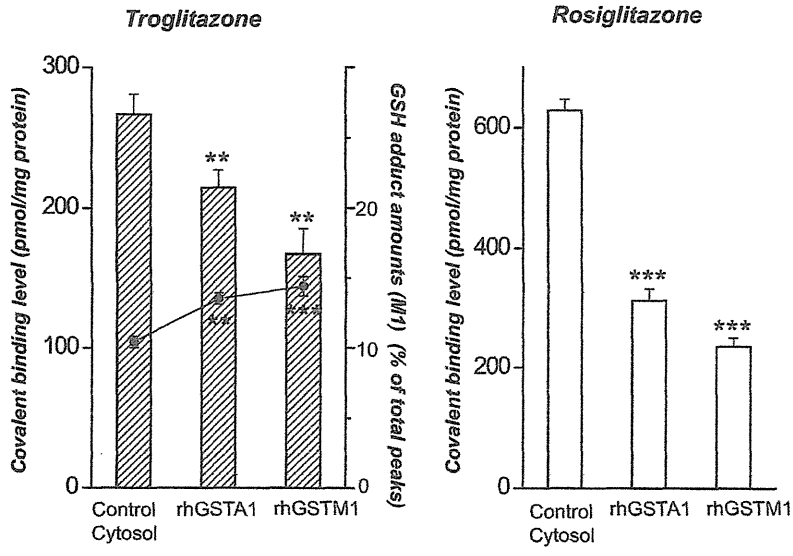

FIG. 2. Effect of rhGSTA1 or rhGSTM1 on CBLs and a GSH adduct in human liver microsomes. Radiolabeled troglitazone and rosiglitazone (10 μM) were incubated with pooled human liver microsomes and with control cytosol (isolated from *E. coli* host strain, left bars), rhGSTA1 (recombinant human GSTA1 expressed in *E. coli*, middle bars), or rhGSTM1 (right bars) in the presence of 1 mM NADPH and 1 mM GSH at 37°C for 1 h followed by determination of CBLs. The eluates were analyzed by radio-HPLC, and the amounts of M1 (the main GSH adduct of troglitazone in this assay) are shown (●). No appreciable GSH adducts of rosiglitazone were found with radio-HPLC. The CBL and GSH adduct data are the means ± S.D. from three assays. **, $p < 0.01$; ***, $p < 0.001$, significantly different from control cytosol.

DRUG METABOLISM AND DISPOSITION
DMD
aspet
Downloaded from dmd.aspetjournals.org at Kanazawa Univ Yakugakubu Lib on June 25, 2011

95% air- 5% CO_2 in 300-μl suspensions of hepatocytes in incubation medium (XenoTech, LLC).

Measurement of CBL. CBL was measured according to the method we reported previously (Usui et al., 2009). Reactions of microsomes and hepatocytes were stopped by addition of ice-cold methanol. For measurement of radioactivity bound to proteins, the reaction mixtures after precipitation were loaded onto glass fiber filters and washed with 80% (v/v) methanol and acetonitrile to remove unbound radioactivity. The first filtrate was used for radio-high-performance liquid chromatography (HPLC) analysis or liquid chromatography (LC)-tandem mass spectrometry (MS/MS) analysis of metabolites unbound to proteins as described below. The filter was transferred to a scintillation vial with 10% SDS and incubated overnight at 55°C to dissolve proteins. The radioactivity and protein concentration were then measured. The CBL was calculated from the following equation:

$$\frac{\text{Radioactivity in the protein solution (dpm/ml)}}{\text{Specific radioactivity of substrate (dpm/pmol)}} \times \text{Protein concentration in the protein solution (mg/ml)}$$

Radio-HPLC and LC-MS/MS Analyses. The first filtrate from the glass fiber filters was collected and evaporated to dryness, and the residue was dissolved in the mobile phase and loaded onto an Inertsil ODS-3 column (3-μm, 2.1 i.d. × 150 mm; GL Science, Inc., Tokyo, Japan) with a column temperature of 40°C. The LC system consisted of an Agilent 1200 (Agilent Technologies, Santa Clara, CA) pump set at a flow rate of 0.25 ml/min. The mobile phase to detect GSH adducts of troglitazone consisted of a linear gradient of solvent A (0.1% formic acid) and solvent B (acetonitrile) according to the following program: 20% B (0 min) to 30% B (5 min) to 35% B (26 min) to 100% B (30 min). The mobile phase to investigate metabolite profiling of troglitazone consisted of a linear gradient of solvent A (0.1% formic acid) and solvent B (acetonitrile) according to the following program: 20% B (0 min) to 30% B (5 min) to 35% B (35 min) to 40% B (55 min) to 100% B (65 min). The mobile phase to investigate metabolite profiling of rosiglitazone consisted of a linear gradient of solvent A (10 mM ammonium acetate) and solvent B (acetonitrile) according to the following program: 5% B (0 min) to 35% B (20 min) to 60% B (35 min) to 100% B (40 min). Radioactivity was detected with a flow scintillation detector (Radiomatic 610TR; PerkinElmer Life and Analytical Sciences, Waltham, MA), using Ultima Flo-M scintillation cocktail (PerkinElmer Life and Analytical Sciences). Mass analysis was conducted on a 4000 QTRAP hybrid triple quadrupole-linear ion trap mass spectrometer (Applied Biosystems, Foster City, CA) equipped with an electrospray ion source for detection of GSH adducts of troglitazone, M1 and M2 (Fig. 1). Ionization parameters included an ion spray voltage of −4100 V and source temperature of 200°C. M1 and M2 were identified by means of multiple reaction monitoring (MRM) in the negative ion mode [MRM transitions: M1, $[M - H]^-$ (deprotonated molecule) = 745 → 272; M2, $[M - H]^-$ = 779 → 272]. MRM parameters of M1 and M2 included a declustering potential of −60 V and collision energy of −35 V. Molecular masses of other metabolites of troglitazone and rosiglitazone were determined as described in our previous article (Usui et al., 2009).

Measurement of ATP Levels in Hepatocytes. Troglitazone and rosiglitazone were incubated with cryopreserved human hepatocytes (1×10^5 cells/ml) genotyped for GSTM1 and GSTT1 at 37°C for 2 h under an atmosphere of 95% air-5% CO_2 in 100-μl suspensions of hepatocytes in incubation medium (XenoTech, LLC). ATP levels were measured using a CellTiter-Glo Luminescent cell viability kit from Promega (Madison, WI). This assay generates luminescent signals by luciferase reactions that are proportional to the amount of ATP present.

Statistical Analysis. All statistical analyses were performed using SAS Enterprise Guide 4.1 (SAS Institute, Cary, NC). Correlations between CBLs or unchanged drug amounts and specific P450 activities in human liver microsomes or hepatocytes were analyzed using linear regression analysis. The two-way analyses of variance were used to test the effect of the GSTM1 genotype and GSTT1 genotype on CBLs or on remaining unchanged drug amounts. Student's *t* test was used to compare the cytotoxicity of troglitazone and rosiglitazone between GSTM1/GSTT1 null and wild-type hepatocytes and to compare the CBL or M1 amounts with addition between rhGSTs and control cytosol.

Results

Correlation between CBLs and P450 Activities of Human Liver Microsomes from Individuals. CBLs of troglitazone and rosiglitazone with 16 individual human liver microsomes phenotyped for enzymatic activities of P450s were investigated in the presence of 1 mM GSH. The average absolute values were 297 and 435 pmol/mg protein, respectively. Despite addition of GSH as a scavenger, individual microsomes showed large variation in CBLs. Compared with the individual CBLs of troglitazone (152–529 pmol/mg), those of rosiglitazone (141–1013 pmol/mg) varied more widely. The coefficient of variation of CBL was 38% for troglitazone and 46% for rosiglitazone. Correlations between CBLs and P450 activities are shown in Table 1. CBLs of troglitazone were significantly and positively correlated with CYP3A activities ($r = 0.89$, $p < 0.001$, testosterone 6β-hydroxylation; $r = 0.83$, $p < 0.001$, midazolam 1′-hydroxylation). Furthermore, CBLs of troglitazone were also positively correlated with CYP2C8 activities ($r = 0.60$, $p = 0.01$). Meanwhile, CBLs of rosiglitazone were significantly and positively correlated with CYP2C8 activities ($r = 0.65$, $p = 0.005$).

TABLE 1

Correlation between CBLs and P450 activities of human liver microsomes from 16 individuals

Radiolabeled troglitazone and rosiglitazone (10 μM) were incubated with 16 individual human liver microsomes in the presence of 1 mM NADPH and 1 mM GSH at 37°C for 1 h followed by determination of CBLs. Experiments were conducted in duplicate and correlation (*R*) between the means of CBLs and P450 activities was analyzed.

P450 Activities	*R* value (*p*)	
	CBLs of Troglitazone	CBLs of Rosiglitazone
CYP1A2 (7-ethoxyresorufin O-dealkylation)	0.08 (0.76)	0.09 (0.73)
CYP1A2 (phenacetin O-deethylation)	0.27 (0.30)	0.10 (0.69)
CYP2A6 (coumarin 7-hydroxylation)	0.22 (0.40)	0.0002 (0.99)
CYP2B6 (*S*-mephenytoin N-demethylation)	0.51 (0.05)	0.18 (0.50)
CYP2B6 (bupropion hydroxylation)	0.31 (0.23)	0.08 (0.76)
CYP2C8 (paclitaxel 6α-hydroxylation)	0.60 (0.01)*	0.65 (0.005)**
CYP2C9 (diclofenac 4′-hydroxylation)	0.05 (0.86)	0.11 (0.67)
CYP2C19 (*S*-mephenytoin 4′-hydroxylation)	0.16 (0.55)	−0.05 (0.85)
CYP2D6 (dextromethorphan O-demethylation)	0.37 (0.14)	0.06 (0.82)
CYP2E1 (chlorzoxazone 6-hydroxylation)	−0.02 (0.94)	0.04 (0.87)
CYP3A4/5 (testosterone 6β-hydroxylation)	0.89 (<0.001)***	0.24 (0.36)
CYP3A4/5 (midazolam 1′-hydroxylation)	0.83 (<0.001)***	0.21 (0.43)
CYP4A11 (lauric acid 12-hydroxylation)	0.07 (0.80)	0.39 (0.13)

* Significant at $p < 0.05$.
** Significant at $p < 0.01$.
*** Significant at $p < 0.001$.

DMD DRUG METABOLISM AND DISPOSITION aspet
Downloaded from dmd.aspetjournals.org at Kanazawa Univ Yakugakubu Lib on June 25, 2011

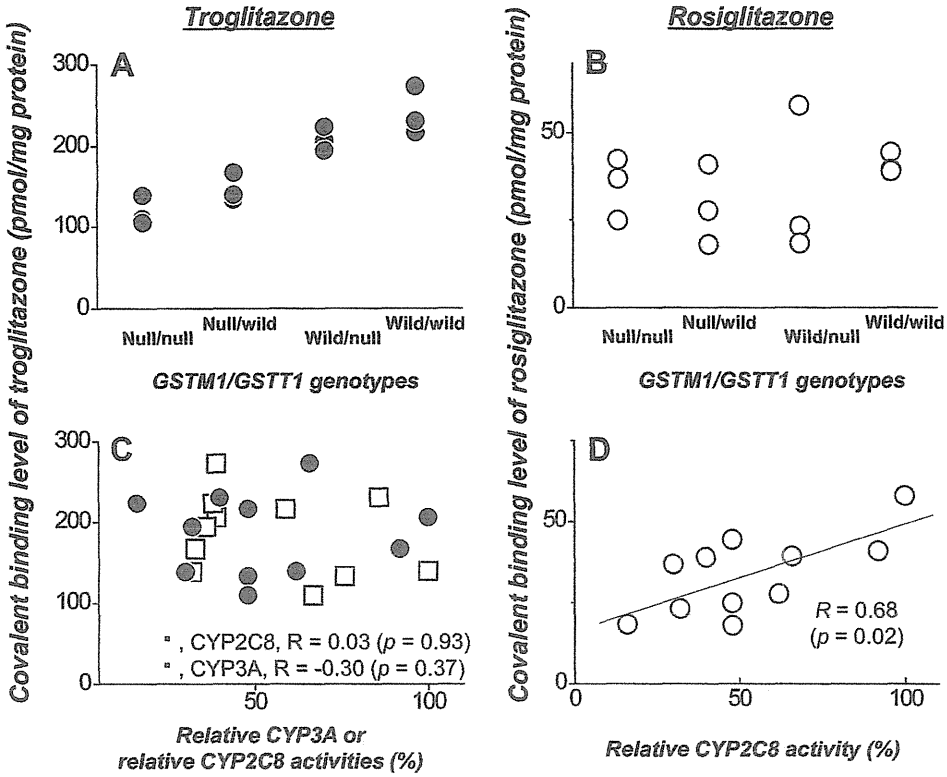

FIG. 3. Comparison of CBLs in GSTM1/GSTT1 null and wild-type hepatocytes. Radiolabeled troglitazone (A and C) and rosiglitazone (B and D) (10 μM) were incubated with 12 cryopreserved human hepatocytes genotyped for GSTM1 and GSTT1 null mutations and phenotyped for P450 activity at 37°C for 8 h followed by determination of CBLs. Two-way analysis of variance results for GSTM1 genotype and for GSTT1 genotype affecting CBLs were shown in Table 3.

Effects of rhGSTA1 or rhGSTM1 on CBLs in Human Liver Microsomes. The scavenging effects of rhGSTA1 or rhGSTM1 (from Cypex Ltd.) on CBLs of troglitazone and rosiglitazone mediated by pooled human liver microsomes were investigated in the presence of 1 mM GSH (Fig. 2). With addition of rhGSTA1 or rhGSTM1, microsomal CBLs of troglitazone and rosiglitazone were significantly decreased compared with those after addition of control cytosol. Furthermore, the GSH adduct of a troglitazone-reactive metabolite reported as 5-glutathionyl-thiazolidine-2,4-dione (M1, Fig. 1) in a previous publication (He et al., 2004) was increased by addition of rhGSTA1 or rhGSTM1 in radio-HPLC analysis (A representative radiochromatogram of troglitazone is shown in Supplemental Fig. 1A.) rhGSTA1 and rhGSTM1 did not affect the decrease in unchanged troglitazone in radio-HPLC analysis (data not shown). Meanwhile, no appreciable GSH adducts of rosiglitazone were found in radio-HPLC.

Correlation between CBLs and GSTM1/GSTT1 Genotypes in Individual Human Hepatocytes. Fifty-nine individual human hepatocytes were genotyped for GSTM1 and GSTT1 null mutations. Three each were selected for each of the four genotypes of GSTM1/GSTT1 (wild/wild, wild/null, null/wild, and null/null) (total 12 lots). With use of the genotyped 12 individual human hepatocytes, CBLs of troglitazone and rosiglitazone were investigated (Fig. 3). Characterizations of individual hepatocytes regarding drug-metabolizing enzymes are shown in Table 2. CBLs of troglitazone were higher than those of rosiglitazone in most of the hepatocytes used (Fig. 3, A and B). CBLs of troglitazone varied widely and independently of the activities of CYP3A and CYP2C8 (Fig. 3C), which are involved in reactive metabolite formation of troglitazone in microsomes (Table 1). CBLs of rosiglitazone in hepatocytes correlated with CYP2C8 activities (r = 0.68, p = 0.02) (Fig. 3D). In contrast to the result of a microsomal assay using rhGSTM1, CBLs of troglitazone in GSTM1 or GSTT1 null hepatocytes tended to be lower than those in GSTM1 or GSTT1 wild-type hepatocytes (Fig. 3A). As the result of two-way analyses of variance to consider the interaction term (Table 3), both the GSTM1 genotype and GSTT1 genotype significantly affected CBLs of troglitazone (F = 54.73, $p < 0.001$ and F = 6.44, p = 0.03, respectively) without the interaction term. On the other hand, neither GSTM1genotype nor GSTT1 genotype significantly affected CBLs of rosiglitazone (F = 0.47, p = 0.51 and F = 0.02, p = 0.90, respectively) without the interaction term.

Correlation between Remaining Unchanged Drugs and GSTM1/GSTT1 Genotypes in Individual Human Hepatocytes. Remaining unchanged drug amounts of troglitazone and rosiglitazone were investigated by radio-HPLC analysis from filtrates after an 8-h incubation with 12 individual human hepatocytes. Representative radiochromatograms of troglitazone and rosiglitazone are shown in Supple-

TABLE 2

Characterization of individual hepatocytes for drug-metabolizing enzymes in the CBL determination assay (lots A–L) and the cytotoxicity assay (lots A, B, J, and K)

Activities of CYP3A (formation rate of 6β-hydroxylated testosterone), CYP2C8 (4'-methylhydroxyl tolbutamide), SULT (7-hydroxycoumarine sulfate), and UGT (7-hydroxycoumarine glucuronide) were measured by the suppliers.

Lot	GSTM1/GSTT1 Genotypes	Enzymatic Activity			
		CYP3A	CYP2C8	SULT	UGT
		pmol/10^6 cell/min			
A	Wild/wild	152	24	31	129
B	Wild/wild	100	33	9	109
C	Wild/wild	223	20	16	432
D	Wild/null	102	50	9	108
E	Wild/null	94	16	110	415
F	Wild/null	99	8	29	444
G	Null/wild	197	24	33	540
H	Null/wild	259	31	34	508
I	Null/wild	85	46	8	86
J	Null/null	174	24	42	366
K	Null/null	82	15	14	118
L	Null/null	188	No data	No data	No data

DRUG METABOLISM AND DISPOSITION DMD aspet
Downloaded from dmd.aspetjournals.org at Kanazawa Univ Yakugakubu Lib on June 25, 2011

TABLE 3

Two-way analysis of variance results for GSTM1 genotype and for GSTT1 genotype affecting CBLs of troglitazone and rosiglitazone

Source	Troglitazone			Rosiglitazone		
	Mean Square	*F*	*p*	Mean Square	*F*	*p*
GSTM1	25034.5	57.43***	<0.001	80.6	0.47	0.51
GSTT1	2806.0	6.44*	0.03	2.9	0.02	0.90
Interaction	7.2	0.02	0.90	139.4	0.81	0.39

* Significant at $p < 0.05$.
*** Significant at $p < 0.001$.

mental Fig. 1, B and C. Remaining unchanged troglitazone amounts in GSTM1 null hepatocytes tended to be higher than those in GSTM1 wild-type hepatocytes (Fig. 4A). As shown by two-way analyses of variance (Table 4), the GSTM1 genotype significantly affected remaining unchanged troglitazone amounts ($F = 8.25$, $p = 0.02$) without the interaction term. The remaining unchanged troglitazone amounts between GSTT1 null and wild-type hepatocytes were not significantly different ($F = 2.85$, $p = 0.13$). On the other hand, neither the GSTM1genotype nor the GSTT1 genotype significantly affected remaining unchanged rosiglitazone amounts ($F = 0.00$, $p = 0.99$ and $F = 2.54$, $p = 0.15$, respectively) without the interaction term (Fig. 4B; Table 4). The stability of [^{14}C]troglitazone and [^{14}C]rosiglitazone under these assay conditions was investigated by radio-HPLC. Troglitazone and rosiglitazone were stable at 10 or 50 μM in hepatocyte incubation medium for 8 h. Saha et al. (2010) reported that troglitazone sulfate was stable under conditions similar to those in our study, and thus troglitazone sulfate was not considered to be deconjugated to unchanged troglitazone.

Troglitazone GSH Adducts (M1 and M2) in GSTM1- and GSTT1-Genotyped Hepatocytes and Substrate Selectivity for the GSH Adducts with the GST Isoforms. GSH adducts of troglitazone were detected by LC-MS/MS analysis from filtrates after incubation with 12 individual human hepatocytes genotyped for GSTM1 and GSTT1 (Fig. 5). The most notable, M1, was identified with all genotypes. However, M2, which is a GSH conjugate of isocyanate or isothiocyanate, the latter involving a novel oxidative scission of the thiazolidinedione ring system (Fig. 1) (Kassahun et al., 2001), was scarcely obtained with GSTM1 null hepatocytes. No appreciable GSH adducts of rosiglitazone were found with any of the genotypes in this study. The substrate selectivity for troglitazone-reactive metabolites trapped as M1 or M2 was verified by incubation of troglitazone with human liver microsomes using rhGSTA1, rhGSTM1, and rhGSTP1 from PanVera Corp. in the presence of 1 mM GSH. LC-MS/MS analysis for detection of GSH adducts, M1 and M2, by means of the MRM method showed that all isoforms (rhGSTA1, rhGSTM1, and rhGSTP1) increased the formation of M1. On the other hand, only rhGSTM1 increased the formation of M2 (Supplemental Fig. 2).

Cytotoxicity Assays in Individual Human Hepatocytes. Data for ATP levels in individual cryopreserved human hepatocytes, genotyped for GSTM1 and GSTT1, after treatment with troglitazone and rosiglitazone are summarized in Fig. 6. CYP3A and CYP2C8 activities, which affect reactive metabolite formation of troglitazone and rosiglitazone (Table 1), were comparable among the hepatocytes in this assay (Table 2). Treatment of GSTM1 and GSTT1 null hepatocytes with 50 μM troglitazone markedly reduced ATP levels compared with those for the no drug control. In contrast, no such reduction was evident in GSTM1 and GSTT1 wild-type hepatocytes exposed to troglitazone. ATP depletion was independent of UDP-glucuronosyltransferase (UGT) and sulfotransferase (SULT) activities (Table 2). Rosiglitazone did not change the cellular ATP concentration with any of the genotypes.

Discussion

"Metabolic idiosyncrasy" and/or "immune idiosyncrasy" are believed to cause DILI (Uetrecht, 2009). Troglitazone-induced liver injury that is not associated with any fever, rash, eosinophilia, or antidrug antibodies (nonallergic hepatotoxicity) has been considered to belong to the category of metabolic idiosyncrasy. Interindividual differences in drug-metabolizing enzymes derived from polymorphisms that lead to greater exposure to reactive metabolites may be one possible explanation for the idiosyncratic nature of this nonallergic hepatotoxicity (Russmann et al., 2010). Conventional animal experiments would not be expected to be able to reproduce troglitazone hepatotoxicity because of the lack of the genetic variation. In this study, we focused on the metabolic idiosyncrasy of troglitazone hepatotoxicity and tried to investigate the mechanism with human in vitro samples featuring high genetic diversity.

In 16 individual microsomal experiments, CBLs of troglitazone were significantly correlated with CYP3A or CYP2C8 activities despite addition of GSH, which is a scavenger of reactive metabolites (Table 1). Our results are in line with the previous report of formation of troglitazone reactive metabolites through oxidation by CYP3A (Kassahun et al., 2001; Tettey et al., 2001; Yamamoto et al., 2002; He et al., 2004). However, CBLs of rosiglitazone were also significantly correlated with CYP2C8 activities, and both the absolute values and the variability were greater than with troglitazone. Therefore, the risk of reactive metabolite formation alone may not explain the clinical outcomes of troglitazone hepatotoxicity.

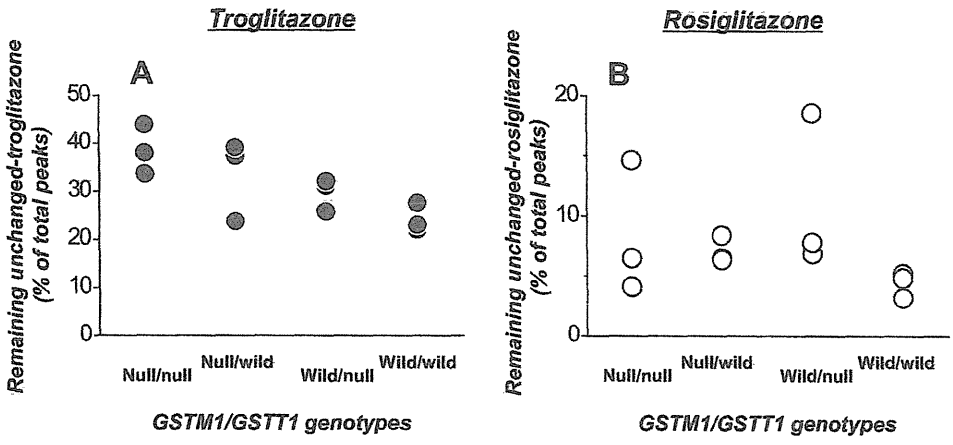

FIG. 4. Comparison of remaining unchanged drug amounts in GSTM1/GSTT1 null and wild-type hepatocytes. Radiolabeled troglitazone (A) and rosiglitazone (B) (10 μM) were incubated with 12 cryopreserved human hepatocytes genotyped for GSTM1and GSTT1 null mutations and phenotyped for P450 activity at 37°C for 8 h followed by radio-HPLC analysis of remaining unchanged troglitazone and rosiglitazone. Two-way analysis of variance results for GSTM1 genotype and for GSTT1 genotype affecting unchanged drug amounts are shown in Table 4.

DMD DRUG METABOLISM AND DISPOSITION aspet
Downloaded from dmd.aspetjournals.org at Kanazawa Univ Yakugakubu Lib on June 25, 2011